HIV Triggers a cGAS-Dependent, Vpu- and Vpr-Regulated Type I Interferon Response in CD4 + T Cells

Jolien Vermeire, Ferdinand Roesch, Daniel Sauter, Réjane Rua, Dominik Hotter, Hanne Vanderstraeten, Anouk van Nuffel, Evelien Naessens, Veronica Iannucci, Alessia Landi, et al.

Article

Cell Reports

HIV Triggers a cGAS-Dependent, Vpu- and Vpr-Regulated Type I Interferon Response in CD4$^+$ T Cells

Graphical Abstract

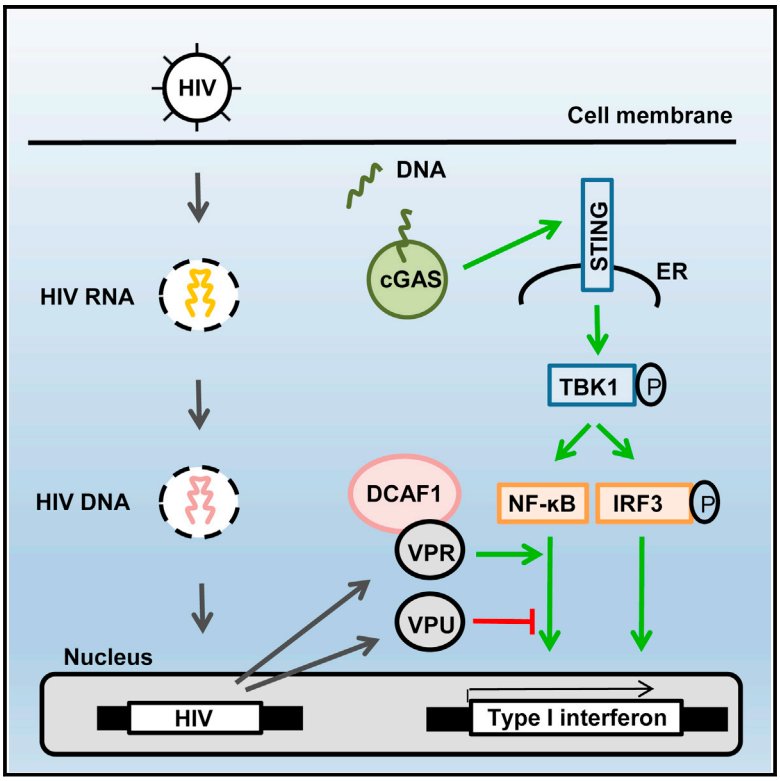

Highlights

- HIV infection triggers a type I interferon (IFN-I) response in primary CD4$^+$ T cells
- IFN-I induction requires integration of HIV-1 and is mediated by cGAS
- HIV-1 Vpr potentiates and Vpu suppresses IFN-I induction

Authors

Jolien Vermeire, Ferdinand Roesch, Daniel Sauter, ..., Ann Baeyens, Frank Kirchhoff, Bruno Verhasselt

Correspondence

bruno.verhasselt@ugent.be

In Brief

Vermeire et al. show that the cytosolic DNA receptor cGAS senses HIV-1 infection and induces type I interferon (IFN-I) production in primary CD4$^+$ T cells. Effective IFN-I induction requires proviral integration and expression of the HIV protein Vpr, while Vpu counteracts cGAS-mediated innate immune activation.

Vermeire et al., 2016, Cell Reports *17*, 413–424
October 4, 2016
http://dx.doi.org/10.1016/j.celrep.2016.09.023

Cell Reports
Article

HIV Triggers a cGAS-Dependent, Vpu- and Vpr-Regulated Type I Interferon Response in CD4$^+$ T Cells

Jolien Vermeire,[1,4] Ferdinand Roesch,[2,4] Daniel Sauter,[3] Réjane Rua,[2,5] Dominik Hotter,[3] Anouk Van Nuffel,[1] Hanne Vanderstraeten,[1] Evelien Naessens,[1] Veronica Iannucci,[1] Alessia Landi,[1] Wojciech Witkowski,[1] Ann Baeyens,[1] Frank Kirchhoff,[3] and Bruno Verhasselt[1,6,*]

[1]Department of Clinical Chemistry, Microbiology, and Immunology, Ghent University, 9000 Ghent, Belgium
[2]Département de Virologie, Unité Virus et Immunité, Institut Pasteur, 75015 Paris, France
[3]Institute of Molecular Virology, Ulm University Medical Center, 89081 Ulm, Germany
[4]Present address: Division of Human Biology, Fred Hutchinson Cancer Research Center, Seattle, WA 98109, USA
[5]Present address: National Institute of Neurological Disorders and Stroke, National Institutes of Health, Bethesda, MD 20892, USA
[6]Lead Contact
*Correspondence: bruno.verhasselt@ugent.be
http://dx.doi.org/10.1016/j.celrep.2016.09.023

SUMMARY

Several pattern-recognition receptors sense HIV-1 replication products and induce type I interferon (IFN-I) production under specific experimental conditions. However, it is thought that viral sensing and IFN induction are virtually absent in the main target cells of HIV-1 in vivo. Here, we show that activated CD4$^+$ T cells sense HIV-1 infection through the cytosolic DNA sensor cGAS and mount a bioactive IFN-I response. Efficient induction of IFN-I by HIV-1 infection requires proviral integration and is regulated by newly expressed viral accessory proteins: Vpr potentiates, while Vpu suppresses cGAS-dependent IFN-I induction. Furthermore, Vpr also amplifies innate sensing of HIV-1 infection in Vpx-treated dendritic cells. Our results identify cGAS as mediator of an IFN-I response to HIV-1 infection in CD4$^+$ T cells and demonstrate that this response is modulated by the viral accessory proteins Vpr and Vpu. Thus, viral innate immune evasion is incomplete in the main target cells of HIV-1.

INTRODUCTION

Type I interferons (IFN-I) are key players in the innate immune response against viral pathogens. They comprise a group of heterogeneous cytokines, including different subtypes of IFN-α and IFN-β. Production of IFN-I is induced through recognition of specific viral products by various pattern-recognition receptors. IFN-I proteins mediate their antiviral effects by stimulating transcription of numerous immunomodulatory and antiviral interferon-stimulated genes (ISGs). In recent years, different ISGs with profound activity against HIV-1, such as the restriction factors APOBEC3G, TRIM5α, BST2/tetherin, and SAMHD1 and the resistance factor MX2, have been identified (Merindol and Berthoux, 2015). In HIV-1-infected patients, serum levels of IFN-I are elevated throughout the course of infection (Hardy et al., 2013). Although IFN-I responses initially limit viral spread, prolonged exposure to IFN-I in the chronic phase of HIV-1/SIV (simian immunodeficiency virus) infection is associated with desensitization and/or detrimental hyper-immune activation and thus contributes to disease progression (Sivro et al., 2014). This paradox was clearly illustrated in SIVmac-infected rhesus macaques, where both in vivo blockage of IFN-I receptors and prolonged treatment with IFN-I accelerated disease progression (Sandler et al., 2014).

Plasmacytoid dendritic cells (pDCs) are known to produce high levels of IFN-I in response to HIV-1 upon recognition of HIV-1 RNA by TLR7 (Lepelley et al., 2011). During acute infection, they are most likely the main source of IFN-I (Kader et al., 2013). However, levels of circulating pDCs, as well as their capacity to produce IFN-I, decrease during progressive infection, suggesting that other cell types also contribute to IFN-I production, particularly during the chronic phase of HIV-1 infection (Nascimbeni et al., 2009). The nature of these IFN-I-producing cell populations remains, however, unclear.

Besides TLR7, other pattern-recognition receptors, such as the DNA sensors cGAS and IFI16, also recognize HIV-1 replication products (Gao et al., 2013; Jakobsen et al., 2013). Several studies have shown that they can be triggered by HIV-1 in certain cell types and experimental conditions, through either pre- (Gao et al., 2013; Monroe et al., 2014) or post-integration (Lahaye et al., 2013) mechanisms. While IFI16 was shown to drive pro-inflammatory responses to HIV-1 in abortively infected resting CD4$^+$ T cells (Monroe et al., 2014) and in macrophages (Jakobsen et al., 2013), cGAS activation by HIV-1 has thus far only been detected in monocyte-derived macrophages (MDMs) and dendritic cells after Vpx treatment or in THP-1 cell lines (Gao et al., 2013; Lahaye et al., 2013). During natural HIV-1 infection, IFN-I induction is thought to be largely absent in HIV-1 target cells as a consequence of effective evasion mechanisms (Rasaiyaah et al., 2013; Yan et al., 2010). Which cell populations

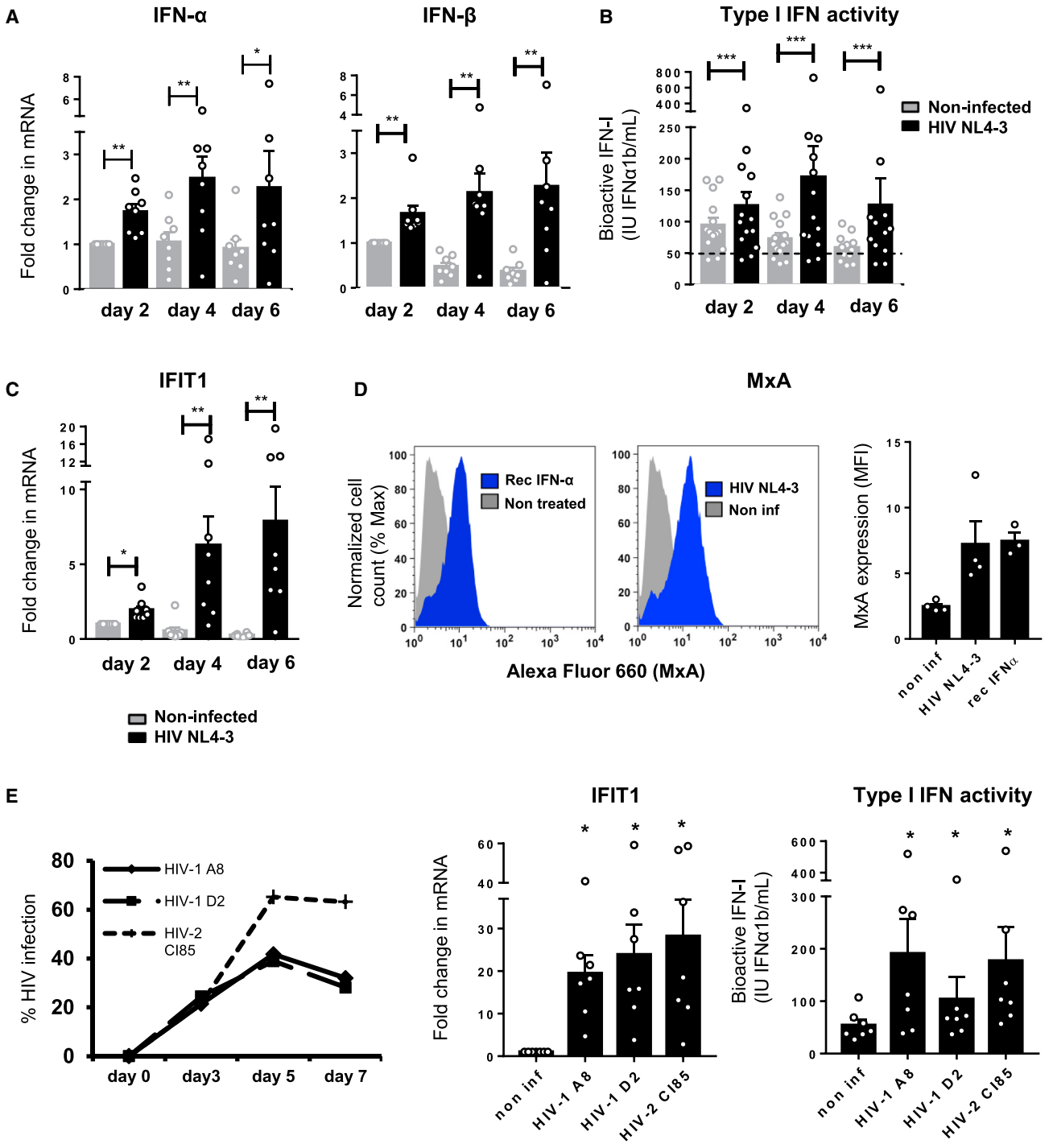

Figure 1. HIV Induces an IFN-I Response in Primary CD4⁺ T Cells

(A) Fold change in IFN-α and IFN-β mRNA levels in primary CD4⁺ T cells infected with HIV-1 NL4-3-GFP-I (black bars) at 2, 4, or 6 days after infection, relative to non-infected (gray bars) cells at day 2 (n = 8).

(B) IFN-I activity in supernatant of cells described in (A). The dashed line corresponds to the detection limit of the assay.

(C) Fold change in *IFIT1* mRNA levels in cells described in (A).

(D) Flow cytometric analysis of non-treated or non-infected cells and primary CD4⁺ T cells treated with recombinant (rec) IFN-α (1,000 IU/mL, IFNα1b) or infected with HIV-1 NL4-3 after intracellular staining for MxA, 3 days after infection or treatment. (Left and Middle) Histograms showing expression of MxA in a representative experiment. (Right) Geometric mean fluorescence intensity (MFI) of MxA expression (n = 3 or 4).

(legend continued on next page)

and sensing pathways contribute to increased levels of IFN-I during chronic HIV-1 infection is currently unclear.

Here, we show that HIV-1 infection can induce a bioactive IFN-I response in activated CD4$^+$ T cells, demonstrating that viral immune evasion is incomplete. IFN-I induction was dependent on proviral integration, indicating that productive infection is required for viral sensing. We identified the cytosolic receptor cGAS as an HIV-1 sensor that induces IFN-I in infected CD4$^+$ T cells. Furthermore, we found that the HIV-1 Vpr protein potentiates the IFN-I response, in both CD4$^+$ T cells and dendritic cells. Conversely, the HIV-1 Vpu protein suppresses cGAS-mediated IFN-I induction, independently of its ability to counteract the restriction factor and innate sensor tetherin. Thus, cGAS-dependent immune sensing of HIV-1 in productively infected activated CD4$^+$ T cells may contribute to the high levels of IFN-I and hyperimmune activation during chronic infection.

RESULTS

HIV Induces an IFN-I Response in Activated Primary CD4$^+$ T Cells

In order to determine if HIV-1 replication induces IFN-I responses in CD4$^+$ T cells, PHA/IL-2 (interleukin-2) activated primary cells were infected with HIV-1 NL4-3 and expression of IFN-I and different ISGs was evaluated (Figure S1A). A significant induction of IFN-α and IFN-β mRNA (Figure 1A) and bioactive IFN-I (Figure 1B) was observed in the HIV-1-infected cultures. CD4$^+$ T cells purified by standard methods contained very few remaining pDCs and additional depletion of pDCs prior to HIV-1 infection excluded them as the source of IFN-I (Figure S1B). While present in all donors, the levels of HIV-1-induced IFN-I mRNA varied in CD4$^+$ T cells derived from different donors and correlated with the percentage of HIV-1-infected cells over time (Figure S1C). Similarly, IFN-I induction correlated with the levels of spreading infection when different inocula of HIV-1 were used (Figure S1D). In addition to IFN-I, multiple ISGs were induced, including *IFIT1* (Figures 1C and S1D) and MxA (MX1) (Figures 1D and S1E) as well as *IFIT3*, *IFI44*, and *OAS1* mRNA and cell-surface BST2 protein (data not shown). The induction of MxA was comparable to that obtained after treatment with recombinant IFN-α (Figure 1D). Infection with two primary HIV-1 group M strains and an HIV-2 isolate also clearly induced *IFIT1* and bioactive IFN-I in primary CD4$^+$ T cells (Figure 1E), confirming that this effect is not restricted to a particular viral strain.

To determine if the IFN-I response induced by HIV-1 in CD4$^+$ T cells suppresses HIV-1 replication, neutralizing antibodies against IFN-α and/or IFN-β were added to infected T cell cultures. In combination, these antibodies markedly decreased induction of the ISG *IFIT1* by HIV-1 (Figure 2A). When added separately, the IFN-α and -β antibodies each enhanced HIV-1 replication to a similar extent. Combining both antibodies had a more potent effect on the fraction of HIV-1-infected cells and also enhanced virus production (Figure 2B). Thus, both IFN-α and -β contribute to the antiviral effect of HIV-induced IFN-I in CD4$^+$ T cells.

HIV-1 Proviral Integration Is Required for IFN-I Induction in Primary CD4$^+$ T Cells

To determine which steps of the HIV-1 replication cycle are required for IFN-I induction, CD4$^+$ T cells were infected with HIV-1 NL4-3 in the presence of reverse-transcriptase (nevirapine) or integrase (raltegravir) inhibitors and compared to cells treated with a protease inhibitor (ritonavir). Inhibition of reverse transcription prevented, and suppression of integration strongly reduced, IFN-I and *IFIT1* mRNA induction by HIV-1. In comparison, strong IFN-I induction was observed when integration was allowed (Figures 3A and S2A). The importance of viral integration was confirmed with an HIV-1 NL4-3 construct containing a D116N mutation that inactivates integrase (Engelman et al., 1995) (Figures 3B and S2B). Since the number of remaining Gag-expressing cells was much lower during infection with HIV-1 D116N compared to infection in the presence of raltegravir (Figures S2A and S2B), remaining levels of integration might account for the modest IFN-I induction by HIV-1 observed in the presence of raltegravir (Figure 3A). Similar to the integrase-deficient virus, a *tat*-defective virus did not significantly induce IFN-I and *IFIT1* mRNA during single-cycle infection of CD4$^+$ T cells (Figures 3C and S2C). Thus, Tat-dependent expression of viral genes, rather than the integration process itself, triggers IFN-I induction in HIV-1-infected primary CD4$^+$ T cells.

IFN-I Induction by HIV-1 in CD4$^+$ T Cells Is Mediated through the cGAS Pathway

To identify host innate sensing pathways triggered by HIV-1 in CD4$^+$ T cells, we performed short hairpin RNA (shRNA)-mediated knockdown studies. Knockdown of the DNA-sensing cGAS receptor in primary CD4$^+$ T cells (Figure 4A) resulted in a marked decrease of *IFIT1* mRNA induction upon HIV-1 infection. The results were confirmed using three independent shRNAs that decreased cGAS expression without affecting cell survival or HIV-1 infection levels (Figures 4B and S3A–S3C). Possibly due to prolonged culture of the primary cells prior to infection, in this experimental set-up HIV-1 infection levels were low (Figure S3A) and IFN-I induction was only detectable in four out of seven donors, even though all of them showed ISG induction and therefore likely produced low levels of IFN-I. In the four donors with a detectable increase in IFN-I, knockdown of cGAS strongly reduced IFN-β induction upon HIV-1 infection (Figure 4C). In comparison, IFN-β and IFIT1 induction were not markedly affected by cGAS knockdown when synthetic cGAMP, the downstream product of cGAS, was used to trigger the IFN-I response (Figure S3D). In monocyte-derived dendritic cells (MDDCs), polyglutamine-binding protein 1 (PQBP1) was recently shown to be required for cGAS-mediated sensing of HIV-1 DNA (Yoh et al., 2015).

(E) Infection levels and IFN-I response in primary CD4$^+$ T cells infected with T-cell-line grown HIV-1 and HIV-2 primary isolates (n = 6). (Left) Percentage of infected cells at different time points after infection, measured by intracellular Gag staining (HIV-1) or by surface CD4 staining (HIV-2). (Middle) Fold change in *IFIT1* mRNA levels 5 days after infection relative to non-infected cells. (Right) IFN-I activity measured in supernatant of cells described above.
Graphs show data and mean (±SEM). *p < 0.05; **p < 0.01; ***p < 0.001 (Wilcoxon matched pairs test was used). See also Figure S1.

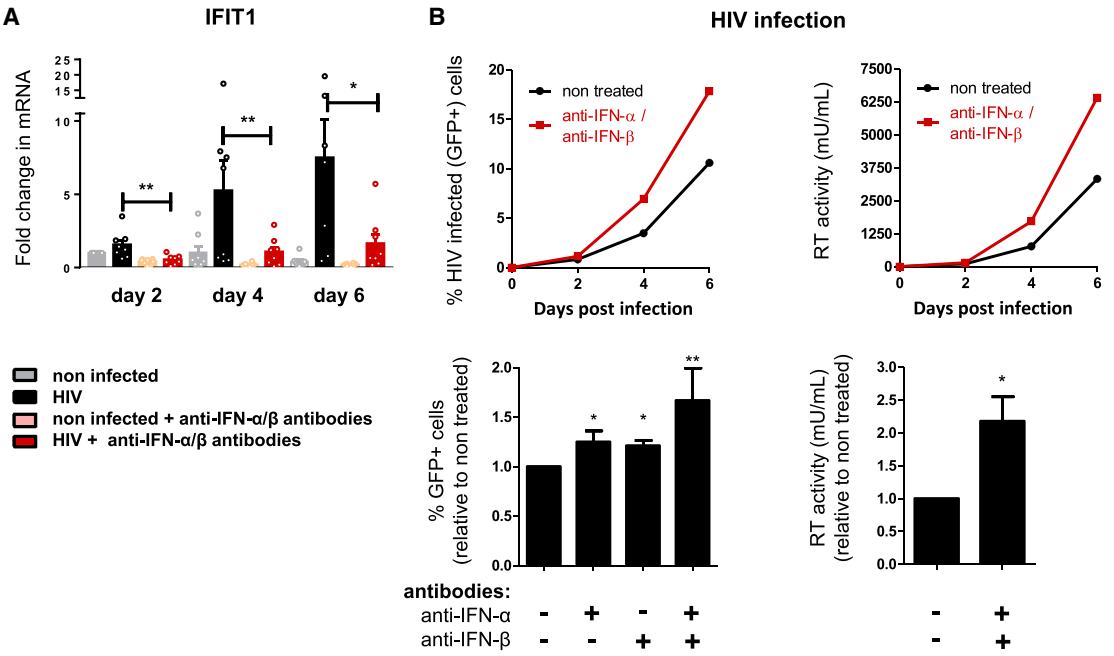

Figure 2. IFN-I Induced by HIV-1 in Primary CD4⁺ T Cells Suppresses Viral Replication

Primary CD4⁺ T cells were infected with HIV-1 NL4-3-GFP-I in the presence or absence of neutralizing antibodies against IFN-α and IFN-β as indicated.
(A) Fold change in *IFIT1* mRNA levels at different time points after infection relative to non-infected non-treated cells at day 2 (n = 7 or 8).
(B) (Top) Percentage of infected cells (GFP+) and reverse-transcriptase (RT) activity in supernatant at different time points (days post infection) in a representative experiment. (Bottom) Percentage of infected cells or RT activity at 4 or 6 days post infection relative to infection in absence of antibodies (n = 6 or 7).
Graphs in (A) show data and mean ± SEM. Graphs in the bottom panels of (B) represent mean ± SEM. *p < 0.05; **p < 0.01. Wilcoxon matched pairs test was used in (A). Kruskal-Wallis ANOVA followed by Dunn's multiple comparisons post hoc test (treated compared to untreated control) was used in the bottom panels of (B).

However, knockdown of PQBP1 in CD4⁺ T cells did not affect the IFN-I induction by HIV-1 (Figure S3E).

To further evaluate involvement of the cGAS pathway in HIV-1-mediated IFN-I induction, we co-cultured shRNA-transduced primary CD4⁺ T cells with HIV-1-infected MT4 T cells (Figure 4D), which allows more efficient virus infection via cell-to-cell transmission (Sourisseau et al., 2007). Co-culture for 24 hr resulted in high levels of HIV-1-infected CD4⁺ T cells and significant IFN-β induction. Importantly, IFN-β induction was not detected in HIV-1-infected MT4 cells cultured alone, or in co-cultures of non-infected MT4 cells and primary CD4⁺ T cells, verifying that HIV-1-infected CD4⁺ T cells are the source of IFN-I (Figure 4E). Inhibition of infection of the primary cells, by addition of replication inhibitors upon co-culture, eliminated IFN-I induction (data not shown). We subsequently performed knockdown of the known cGAS pathway members *MD21D1*/cGAS, *TMEM173*/STING, *TBK1*, and *IRF3* in this experimental setting. Knockdown of cGAS as well as the downstream signaling molecules STING, TBK1, and IRF3 strongly decreased IFN-β induction (Figures 4F, S3F, and S3G). In sum, HIV-1 triggers the cGAS pathway in primary CD4⁺ T cells.

Vpr Potentiates IFN-I Induction by HIV-1

The involvement of cGAS, a DNA sensor, suggests that recognition of reverse-transcribed HIV-1 cDNA is driving the innate immune response to HIV-1 in CD4⁺ T cells. However, our results also indicated that IFN-I induction is dependent on expression of the HIV-1 provirus. Similar to cGAS-mediated sensing of HIV-1 in Vpx-treated (MDDCs), we reasoned that newly expressed viral proteins might be required for IFN-I induction in CD4⁺ T cells. In Vpx-treated MDDCs, HIV-1 DNA sensing is dependent on the interaction of newly expressed HIV-1 capsid (CA) with Cyclophilin A (CypA), which has been suggested to "unmask" HIV-1 DNA for recognition by cGAS (Lahaye et al., 2013; Manel et al., 2010). We used the same panel of HIV-1 CA mutated viruses, complemented with a wild-type (WT) capsid protein during production (Manel et al., 2010). However, viruses expressing capsids that are able (WT, T54A/N57A, Q63A/Q67A) or not (G89V) to interact with CypA induced similar levels of IFN-I (Figure S4A). Thus, IFN-I induction in HIV-1-infected CD4⁺ T cells does not require CypA interaction with newly expressed capsid proteins.

We subsequently evaluated the role of the HIV-1 accessory protein Vpr. This protein was shown to counteract IFN-I responses (Harman et al., 2011; Laguette et al., 2014), but stimulating effects on ISG induction have also been described (Zahoor et al., 2015; Zahoor et al., 2014). We found that *vpr*-defective HIV-1 NL4-3 constructs induced much lower levels of IFN-I and *IFIT1* than the wild-type virus, despite similar infection rates (Figure 5A; Figure S4B), suggesting a potentiating effect of Vpr on innate immune activation. In agreement with previous work (Trotard et al., 2015), the absence of Vpr did not affect or even enhanced the IFN-I response in STING-expressing TZM-bl cells (Figure S4C). Infection of CD4⁺ T cells with *vpr*-defective viruses complemented with WT Vpr during production also induced only

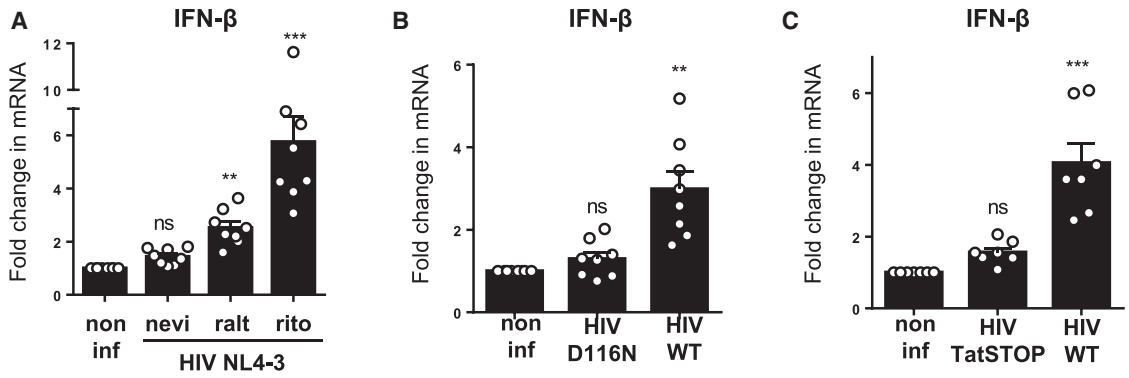

Figure 3. Type I IFN Induction in Primary CD4⁺ T Cells Requires HIV-1 Integration

Fold change in IFN-β mRNA levels relative to non-infected cells in primary CD4⁺ T cells of different donors infected with: (A) HIV-1 NL4-3 in the presence of a reverse transcription inhibitor (nevirapine, nevi), integration inhibitor (raltegravir, ralt), or protease inhibitor (ritonavir, rito) 48 hr after infection (n = 8); (B) HIV-1 NL4-3 wild-type (HIV WT) or D116N integrase mutant (HIV D116N) 24 hr after infection (n = 8); and (C) HIV-1 NL4-3-HSA-I wild-type (HIV WT) or *tat*-defective virus (HIV TatStop) in the presence of ritonavir 48 hr after infection (n = 7). Graphs show data and mean ± SEM. ns, not significant; $^{**}p < 0.01$; $^{***}p < 0.001$. Friedman test followed by Dunn's multiple comparisons post hoc test (infected compared to non-infected control) was used. See also Figure S2.

low levels of IFN-I (Figures 5B and S4D). Thus, de-novo-synthesized, and not virion-incorporated, Vpr is responsible for efficient IFN-I induction, which helps to explain why the IFN-I response occurs post-integration. Reduced IFN-I induction was also observed with an otherwise isogenic HIV-1 construct containing a single Q65R substitution in Vpr, which is known to disrupt binding of Vpr to DCAF1 (DeHart et al., 2007). By contrast, viruses expressing the Vpr R77Q variant, associated with reduced pro-apoptotic activity of Vpr (Lum et al., 2003), induced a potent IFN-I response (Figures 5C and S4E). Knockdown of DCAF1 strongly decreased induction of IFIT1 and IFN-β upon HIV-1 infection (Figure 5D), but did not affect residual IFN-I induction by a *vpr*-defective virus (Figure S4F). Thus, DCAF1 clearly plays a role in the Vpr potentiating effect. A similar result was obtained when cells were treated with an inhibitor of TAK1, a key regulator of the nuclear factor κB (NF-κB) signaling pathway, prior to infection. TAK1 was previously suggested to bind Vpr and be required for Vpr-mediated activation of NF-κB (Liu et al., 2014). The TAK1 inhibitor did not affect cell survival (data not shown) or HIV-1 infection levels but highly decreased IFN-I induction by WT HIV-1. By contrast, remaining induction by a *vpr*-defective virus was not affected, suggesting a Vpr-dependent effect (Figure 5E). Together, these results indicate that de novo synthesized Vpr potentiates the IFN-I response in a DCAF1- and TAK1-dependent fashion.

Given the potentiating effect of Vpr on IFN-I production in activated CD4⁺ T cells, we investigated if Vpr may play a similar role in other immune cells. Myeloid dendritic cells are usually largely resistant to productive HIV-1 infection due to restriction by SAMHD1. However, the addition of viral-like particles (VLPs) carrying Vpx allows HIV-1 infection and promotes cGAS-dependent IFN-I release (Lahaye et al., 2013). Since HIV-1-infected T cells are more potent inducers of IFN-I in MDDCs than cell-free virions (Puigdomènech et al., 2013), we measured bioactive IFN-I levels in co-cultures of Vpx-treated MDDCs and MT4 cells infected with *vpr*-deficient or WT HIV-1 NL4-3 (Figure 5F). MDDCs became productively infected, and similar levels of Gag+ cells were observed with WT or *vpr*-deficient viruses. Although HIV-1 infection of MDDCs was generally associated with IFN-I release, production of type I IFN was strongly reduced in the absence of Vpr (Figure 5G). Thus, Vpr potentiates IFN-I production in both activated CD4⁺ T cells and dendritic cells.

Vpu Suppresses IFN-I Induction by HIV-1 in CD4⁺ T Cells

Finally, we evaluated the role of HIV-1 Vpu in regulating the IFN-I response in CD4⁺ T cells, as several studies have indicated an ability of Vpu to counteract IFN-I induction (Doehle et al., 2012; Galão et al., 2012; Sauter et al., 2015). We indeed found that *vpu*-deleted HIV-1 NL4-3 constructs induced a stronger IFN-I response than WT viruses in primary CD4⁺ T cells (Figure 6A; Figure S5A). Such a suppressive effect of Vpu was suggested to depend on counteraction of the restriction factor and innate sensor tetherin (Galão et al., 2012). However, Vpu is also able to counteract IFN-I induction independently of tetherin by downstream inhibition of NF-κB activation (Hotter et al., 2013; Sauter et al., 2015). To assess whether Vpu's ability to downregulate tetherin plays a role in suppressing the HIV-1-induced IFN-I response in CD4⁺ T cells, we infected cells with HIV-1 NL4-3 viruses containing *vpu* alleles from different primate lentiviruses with varying abilities to antagonize tetherin (Sauter et al., 2009). All these Vpus suppressed the IFN-I response irrespectively of their anti-tetherin activity (Figure 6B; Figure S5B). Notably, an HIV-1 NL4-3 construct containing a mutation in the β-TrCP binding motif of Vpu (S52A) that impairs both anti-tetherin and anti-NF-κB activity (Pickering et al., 2014) lost the ability to suppress the HIV-1-induced IFN-I response (Figure 6B; Figure S5B). We subsequently investigated if cGAS is required for IFN-I induction by *vpu*-deleted viruses. Upon knockdown of cGAS, *vpu*-deleted and WT viruses induced similarly low levels of IFN-β (Figure 6C), suggesting that Vpu dampens the cGAS-dependent IFN-I response to HIV-1 in primary CD4⁺ T cells.

To evaluate the combined effects of Vpu and Vpr on IFN-I induction during HIV-1 infection, CD4⁺ T cells were infected with matched HIV-1 NL4-3 viruses carrying a deletion in *vpr*, *vpu*, or both genes. As both proteins may affect IFN-I induction via the NF-κB pathway, we also investigated the effect of the TAK1

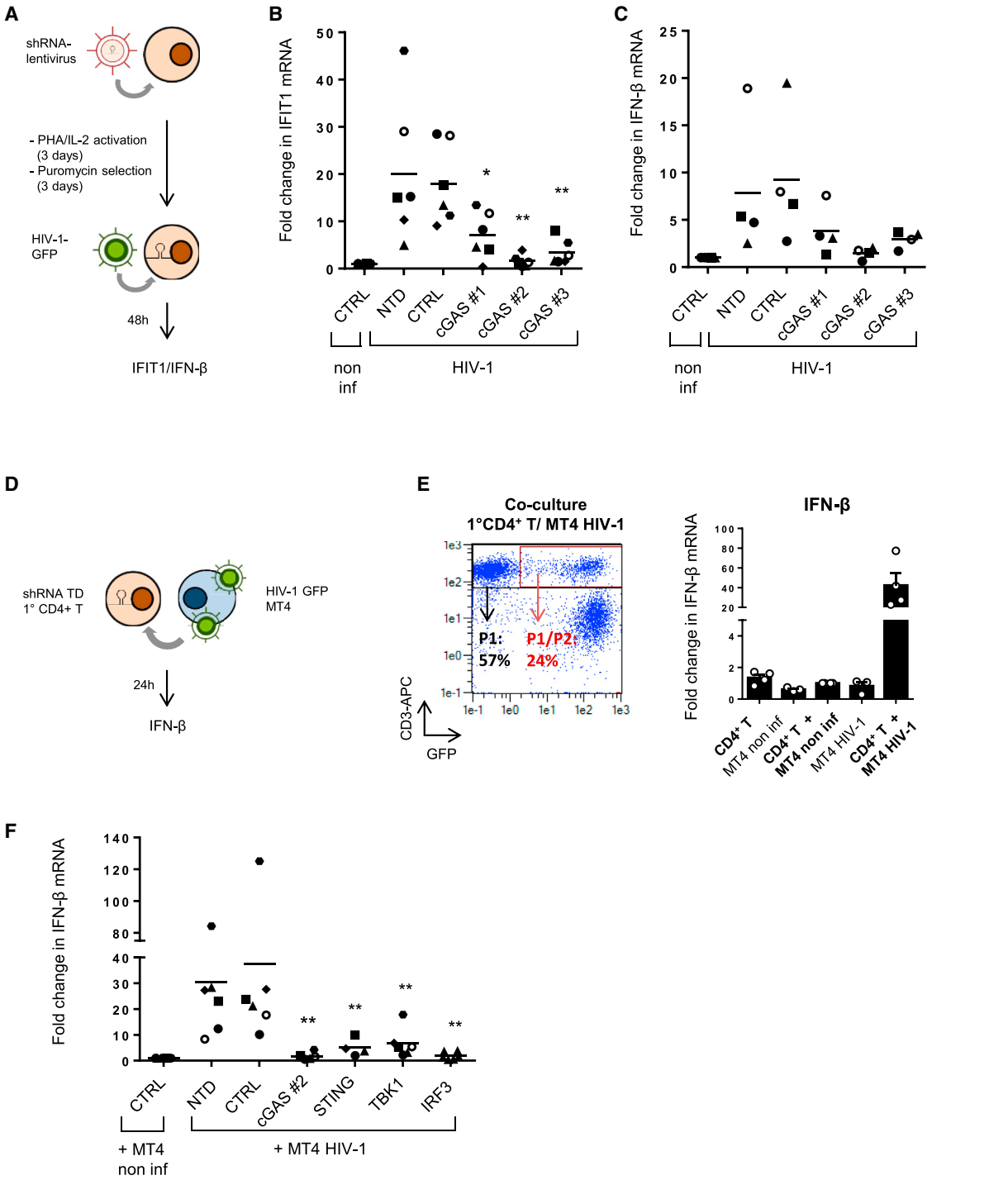

Figure 4. cGAS and Downstream Signaling Molecules Are Required for IFN-I Induction by HIV-1 in Primary CD4⁺ T Cells

(A) Experimental set-up 1 to measure host protein involvement in IFN-I induction by HIV-1: primary CD4⁺ T cells are transduced with pLKO.1 shRNA-encoding vectors and activated with PHA/IL-2 for 3 days, and efficiently transduced cells are selected with puromycin for 3 days. Cells are subsequently infected with HIV-1 NL4-3-GFP-I virus, and *IFIT1*/IFN-β mRNA levels are measured 48 hr after infection.

(B) Fold change in *IFIT1* mRNA levels in HIV-1-infected cells described in (A), relative to non-infected (non inf) cells transduced with a non-targeting shRNA control vector (CTRL). NTD, non-transduced cells. cGAS #1, #2, and #3 are different shRNA sequences targeting cGAS (n = 6).

(C) Fold change in IFN-β mRNA levels in experiments described in (B) with detectable IFN-β induction (n = 4).

(D) Experimental set-up 2: primary CD4⁺ T cells transduced with shRNA-encoding vectors as described in (A) are co-cultured with MT4 cells infected with HIV-1 NL4-3-GFP-I virus. IFN-β mRNA levels are measured 24 hr after the start of co-culture.

(legend continued on next page)

inhibitor on IFN-I induction by these viruses. The *vpr-vpu*-deficient virus induced an IFN-I response that was intermediate between the one triggered by viruses containing individual defects in *vpr* and *vpu* (Figures 6D and S5C). Thus, both accessory proteins can exert their effect on IFN-I induction independently from each other. A similar observation was made upon treatment with the TAK1 inhibitor: in contrast to the *vpr*-deleted virus, the *vpr-vpu*-deficient virus was markedly affected by the inhibitor (Figure 6E and S5D). This supports that Vpu suppresses IFN-I induction through the NF-κB pathway and shows that this effect is particularly important in the presence of the potentiating effect of Vpr on this pathway.

DISCUSSION

In the present study, we demonstrate that activated $CD4^+$ T cells, the main targets for HIV replication in vivo, sense HIV-1 replication products and secrete bioactive IFN-I following induction through a post-integration mechanism involving the cGAS signaling pathway. Furthermore, we show that this response is subject to potentiation by Vpr and counteraction by Vpu. These findings are important, since IFN-I released from $CD4^+$ T cells during the chronic phase of HIV-1 infection may contribute to the detrimental hyper-immune activation that drives progression to AIDS.

Triggering of an innate immune response during wild-type HIV-1 infection of non-manipulated primary cells has thus far only been observed in pDCs and abortively infected resting $CD4^+$ T cells (Doitsh et al., 2014; Lepelley et al., 2011). In our experiments, residual CD14-expressing cells were well below 0.1% (data not shown) and pDCs were virtually eliminated in the purified $CD4^+$ T cell population, arguing against a significant contribution of these myeloid cells to the IFN-I response we measured. Except for two studies showing induction of ISGs (Nasr et al., 2012) or IFN-I (Imbeault et al., 2009), IFN-I production was not observed after HIV-1 infection of the main target of HIV in vivo, activated $CD4^+$ T cells (Doehle et al., 2012; Yan et al., 2010). In the present study, production of IFN-I was considerably enhanced by high HIV-1 infection levels, e.g., during spreading replication, and might be missed in low-level single-round infection studies. In addition, IFN-I induction was absent in MT4 cells (Figure S3F) and other T cell lines (data not shown). These are possible reasons why IFN-I induction in HIV-infected T cells was missed in studies mentioned above.

While the ability of cGAS to sense HIV-1 DNA was previously described, its activation is thought to be evaded under normal infection conditions (Lahaye et al., 2013; Rasaiyaah et al., 2013). An important implication of our findings is that cGAS is not just a silent sensor, but plays an active role during HIV-1 infection and therefore possibly during pathogenesis. In agreement with this, a recent study demonstrated specific activation of cGAS by HIV-1 in conventional dendritic cells derived from elite controllers, possibly due to higher levels of cGAS in these cells (Martin-Gayo et al., 2015). In light of our findings, it will be interesting to evaluate if cGAS expression levels in $CD4^+$ T cells may affect the levels of inflammation and disease outcome.

Our results clearly show that cGAS-mediated sensing occurs after viral integration and requires de novo expression of viral RNA or proteins, since *integrase*- or *tat*-deficient viruses or treatment with an integrase inhibitor strongly reduced IFN-I induction. How can post-integration sensing by cGAS be explained? Two possible scenarios can be envisioned. First, it is possible that newly expressed RNA triggers the cGAS pathway. Protection against RNA virus infection by cGAS expression has been demonstrated (Schoggins et al., 2014), and similar to the DNA sensor PQBP1, hypothetically an RNA co-receptor might exist. A second and more likely explanation is that cGAS recognizes cytosolic DNA. This may be mitochondrial DNA aberrantly released in the cytoplasm as a consequence of mitochondrial stress induced by newly expressed viral proteins, as reported in herpes simplex virus (HSV) infection (West et al., 2015). Notably, several studies have shown that Vpr induces mitochondrial damage (Huang et al., 2012; Jacotot et al., 2001), which might explain its enhancing effect on IFN-I induction in primary $CD4^+$ T cells. Alternatively, cytoplasmic HIV pre-integration complex cDNA could be the pathogen-associated molecular pattern (PAMP) sensed and IFN-I production could be stimulated above a critical threshold by a newly expressed viral protein, e.g., through additional NF-κB activation. These HIV DNA products could originate from either simultaneous or previous abortive infection events. Although further studies will be needed to demonstrate a similar post-integration sensing mechanism during HIV cell-to-cell transmission, it is know that this mode of infection allows for the simultaneous transmission of many virions (Del Portillo et al., 2011; Sigal et al., 2011). Even though most of these will fail to establish productive infection, their reverse-transcription products could be targeted for cGAS detection by a successfully integrated virus. HIV co-infection has been primarily detected in splenic tissues of patients (Gratton et al., 2000; Jung et al., 2002) where B and T lymphocytes, but not pDCs, were found to be the IFN-α producing cells (Nascimbeni et al., 2009). In such niches, cGAS-mediated post-integration sensing could be a driving mechanism for IFN-I production.

(E) (Left) Expression of GFP and CD3 in co-cultures of primary $CD4^+$ T cells ($CD3^{high}$ cells) transduced with an shRNA control vector and MT4 cells infected with HIV NL4-3-GFP-I ($CD3^{low}$ cells), 24 hr after start of co-culture in a representative experiment. P1, % $CD3^{high}$ cells; P1/P2, % GFP+ cells among $CD3^{high}$ cells. (Right) Fold change in IFN-β mRNA levels in cultures of non-infected primary $CD4^+$ T cells transduced with shRNA control vector ($CD4^+$ T), non-infected MT4 cells (MT4 non inf), MT4 cells infected with HIV NL4-3-GFP-I (MT4 HIV-1), or co-cultures of these cells (n = 3 or 4), relative to levels in co-cultures with non-infected MT4 cells.

(F) Fold change in IFN-β mRNA levels in co-cultures of non-infected or HIV-1-infected MT4 cells with primary $CD4^+$ T cells transduced with either vectors encoding shRNA targeting the indicated genes, with the shRNA control vector (CTRL) or non-transduced cells (NTD) (n = 4–6), relative to levels obtained in co-cultures of CTRL cells and non-infected (non inf) MT4 cells.

(B), (C), (E), and (F) show data (data point symbols refer to individual donors) and mean. In (E), data indicate mean ± SEM. *$p < 0.1$; **$p < 0.01$ (Mann-Whitney test). See also Figure S3.

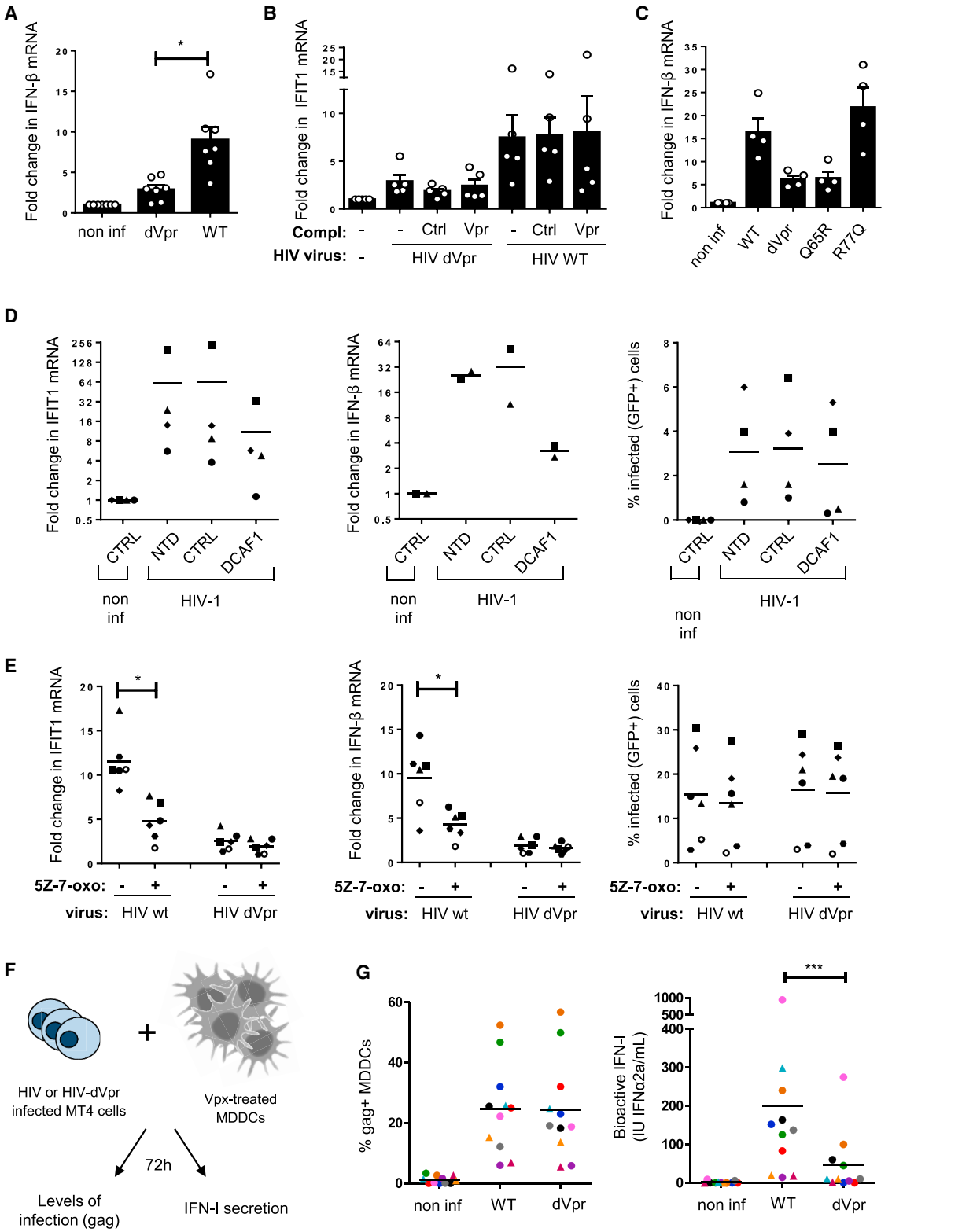

Figure 5. Vpr Potentiates HIV-1-Mediated IFN-I Induction in Primary CD4⁺ T Cells and Dendritic Cells

(A–C) Innate immune response in HIV-1-infected primary CD4⁺ T cells relative to non-infected (non inf) cells.

(A) IFN-β mRNA levels 48–72 hr after infection with HIV-1 NL4-3-HSA-I wild-type (WT) or *vpr*- defective virus (dVpr) (n = 7).

(legend continued on next page)

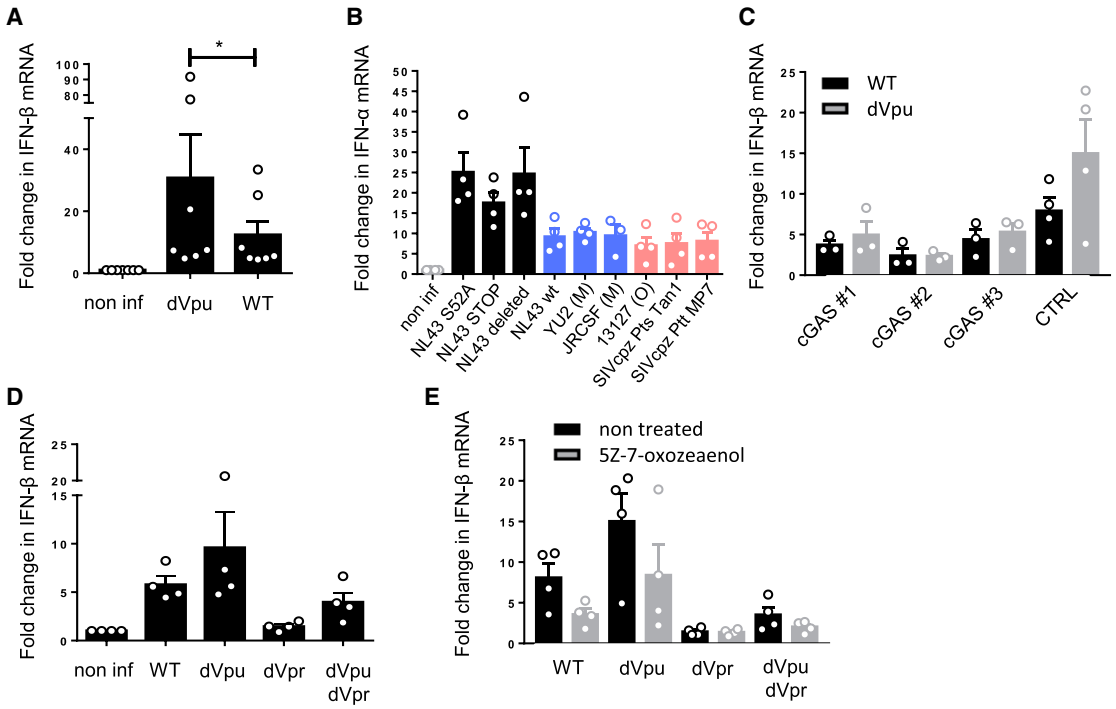

Figure 6. Vpu Suppresses cGAS-Mediated IFN-I Induction in Primary CD4⁺ T Cells

(A–D) IFN-I response in HIV-1-infected primary CD4⁺ T cells relative to non-infected (non inf) cells.

(A) IFN-β mRNA levels 48 hr after infection with VSV-G pseudotyped HIV-1 NL4-3-I-EGFP wild-type (WT) or *vpu*-deleted (dVpu) virus (n = 7).

(B) IFN-α mRNA levels 48 hr after infection with VSV-G pseudotyped HIV-1 NL4-3-Vpu-IRES-Env viruses in which the original *vpu* allele was replaced by the *vpu* allele of the indicated HIV-1 or SIV strain. Black bars show viruses with mutated NL4-3 *vpu* alleles, blue bars show viruses with *vpu* alleles that antagonize human tetherin, red bars show viruses with *vpu* alleles that do not antagonize human tetherin (n = 4).

(C) IFN-β mRNA levels 48 hr after infection with VSV-G pseudotyped HIV-1 NL4-3-I-EGFP wild-type (WT) or *vpu*-deleted (dVpu) virus of cells transduced with either shRNA-encoding lentiviruses targeting cGAS or a non-targeting control vector (CTRL) (n = 3 or 4).

(D) IFN-β mRNA levels 48 hr after infection with VSV-G pseudotyped HIV-1 NL4-3-I-EGFP wild-type (WT), *vpu*-deleted (dVpu), *vpr*-deleted (dVpr), or *vpu*- and *vpr*-deleted (dVpu dVpr) viruses (n = 4).

(E) As described in (D), in the presence or absence of 50 nM of TAK1 inhibitor (5Z)-7-oxozeaenol (n = 6).

Graphs show data and mean ± SEM. *p < 0.05 (Wilcoxon matched pairs test). See also Figure S5.

In Vpx-treated MDDCs, post-integration sensing of HIV-1 cDNA has been reported (Lahaye et al., 2013; Manel et al., 2010). In contrast to MDDCs, in T cells the product that enables the sensing of HIV DNA after integration is not the newly expressed HIV-1 capsid. Rather, we found that newly expressed Vpr is required for full post-integration IFN-I induction since *vpr*-deleted viruses induced lower levels of IFN-I in both CD4⁺ T cells and Vpx-treated MDDCs. Virion complementation experiments indicate that, at least in CD4⁺ T cells, virion-packaged Vpr is insufficient to potentiate IFN-I induction. However, unlike the *integrase* mutant, IFN-I induction by the *vpr*-deleted viruses was not entirely absent in CD4⁺ T cells. Therefore, Vpr is most likely an important, but not the sole, viral factor boosting post-integration IFN-I induction. Our evaluation of *vpr*-mutated

(B) *IFIT1* mRNA levels 48 hr after infection with HIV-1 NL4-3-HSA-I wild-type (WT) or *vpr*- defective (dVpr) viruses, not complemented (-) or complemented with a control vector (Ctrl) or WT Vpr (Vpr) during production. Infection was performed in the presence of ritonavir (n = 5).

(C) IFN-β mRNA levels 3 days after infection with HIV-1 NL4-3 viruses: wild-type (WT), *vpr*- deleted (dVpr), and viruses with Q65R or R77Q mutation in Vpr (n = 4).

(D) *IFIT1* mRNA levels (left), IFN-β mRNA levels (middle), and percentage of HIV-1-infected cells (GFP+) (right) 48 hr after infection with VSV-G pseudotyped HIV-1 NL4-3-I-EGFP wild-type (WT) virus of cells transduced with either shRNA-encoding lentiviruses targeting DCAF1 or a non-targeting control vector (CTRL) or not transduced (NTD) (n = 2 or 4).

(E) *IFIT1* mRNA levels (left), IFN-β mRNA levels (middle), and percentage of HIV-1-infected cells (GFP+) (right) 48 hr after infection with VSV-G pseudotyped HIV-1 NL4-3-I-EGFP wild-type (WT) or *vpr*-defective (dVpr) viruses in the presence or absence of 50 nM of TAK1 inhibitor (5Z)-7-oxozeaenol (n = 6).

(F) Experimental outline: MDDCs were pre-treated with Vpx VLPs to allow productive infection. MT4 cells were infected with HIV-1 NL4-3 wild-type (WT) or *vpr*-deleted (dVpr) viruses and subsequently co-cultured with MDDCs. After 72 hr, supernatant was harvested for quantification of IFN-I and infection was monitored by intracellular Gag staining.

(G) (Left) Percentage of HIV-1-infected MDDCs (Gag+) (n = 11). (Right) IFN-I activity in supernatant of co-cultures (n = 11).

Graphs in (A)–(E) and (G) represent data (data point symbols refer to individual donors) and mean. In (A)–(C), data indicate mean ± SEM. *p < 0.05; ***p < 0.001 (Wilcoxon matched pairs test). See also Figure S4.

viruses and knockdown studies indicates that the interaction of Vpr with DCAF1 is required for this effect. Vpr hijacks DCAF1 to recruit the DDB1-Cul4 E3 ubiquitin ligase complex. This complex is involved in different Vpr functions (Casey et al., 2010). However, activation of the DNA damage response by Vpr is particularly interesting in this regard because of the large overlap and interplay between cellular DNA damage response and activation of NF-κB or IRFs (Chatzinikolaou et al., 2014). We show that IFN-I induction by wild-type HIV-1 but not a *vpr*-deleted derivative is sensitive to inhibition of TAK1, which is consistent with an activating effect of Vpr on NF-κB. As such, it is tempting to speculate that stimulation of IFN-I production by Vpr may be a by-product of a Vpr-host interaction with yet-to-be defined beneficial effects during viral replication, e.g., an indirect effect of the DNA damage response or a direct consequence of NF-κB activation (Liu et al., 2014; Roesch et al., 2015; Roux et al., 2000) to enhance proviral expression.

We also observe a potentiating effect of Vpr on IFN-I induction by HIV-1 infection of Vpx-treated MDDCs as was recently described for MDMs and non-Vpx-treated MDDCs (Zahoor et al., 2014, 2015). In contrast, others showed a suppressive role of Vpr in IFN-I production, either in non-Vpx-treated MDDCs (Harman et al., 2011), in MDMs (Mashiba et al., 2014), or in cell lines, such as HEK293 or HeLa (Doehle et al., 2009; Laguette et al., 2014; Okumura et al., 2008; Trotard et al., 2015). Consistent with these latter reports, we observed a suppressing effect of Vpr on IFN-α induction in HeLa-derived STING-expressing TZM-bl cells. These findings strongly suggest that the outcome of the Vpr effect is cell-type dependent and questions the relevance of cell lines as a model for sensing in activated T cells. While the sensing pathway activated by the (*vpr*-deleted) HIV-1 in these studies is unknown, at least in TZM-bl cells activation seems to occur prior to viral integration (Trotard et al., 2015) and may therefore result from stimuli different from the cGAS-mediated post-integration sensing in $CD4^+$ T cells and Vpx-treated MDDCs (Lahaye et al., 2013). Furthermore, pre-integration sensing implies that the suppressing effect is mediated by virion-packaged Vpr, while we show the newly expressed Vpr to be responsible for potentiation of post-integration sensing.

In line with previous reports (Doehle et al., 2012; Galão et al., 2012; Sauter et al., 2015), we found that Vpu efficiently suppresses IFN-I induction in HIV-1-infected $CD4^+$ T cells. Our results provide insight into the specific sensing pathway targeted by Vpu and provide a rationale as to why a late HIV-1 protein is employed by the virus to counteract IFN-I induction. Indeed, since Vpu is only present in the infected cell after viral integration, it is likely to have evolved as a counteracting factor of a post-integration IFN-I trigger. Here, we show that sensing of *vpu*-deleted viruses is cGAS dependent, indicating partial suppression of cGAS sensing by Vpu rather than suppression of an alternative independent IFN-I inducing pathway. Although it is possible that enhanced tetherin-mediated NF-κB activation contributes to higher IFN-I induction by *vpu*-deleted viruses (Galão et al., 2012), the cGAS dependency indicates that tetherin signaling on its own is likely insufficient to trigger IFN-I production in $CD4^+$ T cells. Furthermore, we show that HIV-1 and SIV isolates known to employ Nef to counteract tetherin use Vpu to suppress HIV-1-mediated IFN-I induction, again pointing to a tetherin-independent function. We and others have demonstrated that Vpu suppresses NF-κB activation in response to various stimuli, a process that is partially mediated by sequestration of β-TrCP by Vpu and stabilization of IκBα (Besnard-Guerin et al., 2004; Bour et al., 2001; Manganaro et al., 2015; Pickering et al., 2014; Sauter et al., 2015). Our results with *vpr*-, *vpu*-, and *vpr-vpu*-deficient viruses suggest that Vpu may counteract NF-κB activation by Vpr and suppress a Vpr-independent trigger of NF-κB activation. Activation of STING is indeed known to induce activation of NF-κB on its own (Kato et al., 2013), and silencing of NF-κB p65 was shown to decrease IFN-β production in response to dsDNA (Abe and Barber, 2014). Therefore, Vpu may dampen IFN-I induction in primary $CD4^+$ T cells by interfering with NF-κB activation, the latter in part due to Vpr-enhanced cGAS-mediated sensing.

Our work provides insight in the virus-host interplay that regulates HIV-1 sensing in its main target cells. Our identification of HIV-1-infected $CD4^+$ T cells as potential contributors to IFN-I production and hence harmful chronic inflammation might provide the basis for novel therapeutic strategies.

EXPERIMENTAL PROCEDURES

Viral constructs, the experimental outline, and applied methods are indicated in the figure legends and explained in detail in the Supplemental Experimental Procedures.

Quantification of IFN-I Responses

IFN-α, IFN-β, and *IFIT1* mRNA levels were measured by qPCR using specific primers as listed in the Supplemental Experimental Procedures. IFN-I biological activity in the supernatant was measured using HL-116 luciferase reporter cells. MxA protein levels were quantified by intracellular staining and flow cytometry.

HIV Proviral Constructs and Infection

HIV-1 NL4-3 derived constructs are listed in the Supplemental Experimental Procedures. Viruses were produced in HEK293T cells, complemented, if indicated, by co-transfection with Gag- or Vpr-expressing plasmids. HIV-1 and HIV-2 isolates were propagated in peripheral blood mononuclear cells (PBMCs) and Jurkat CD4 CCR5 cells. Primary $CD4^+$ T cells, obtained from blood of healthy donors, underwent extra pDC depletion and were infected with HIV by spinoculation using 6–3,000 mU reverse transcriptase of virus per 250,000 cells. Anti-retrovirals, IFN-I neutralizing antibodies, and (5Z)-7-oxozeaenol were added prior to or immediately after spinoculation, respectively, and maintained during culture. Monocytes were isolated from PBMCs and differentiated in the presence of IL-4 and granulocyte-macrophage colony-stimulating factor (GM-CSF). MDDCs were treated with VLPs carrying Vpx and infected with HIV-1 through co-culture with MT4 cells. The HIV-1 group M D2 (VI203) (Louwagie et al., 1993) and HIV-2 CI85 (Arien et al., 2005) strains were previously isolated from patients attending the AIDS clinic at the Institute of Tropical Medicine in Antwerp, Belgium with the approval of the ethical committee after written informed consent.

Knockdown of Host Genes and Co-culture with HIV-1-Infected Cells

The origin and properties of pLKO.1-puro shRNA-encoding lentiviral construct are listed in the Supplemental Experimental Procedures. Lentiviruses were produced in HEK293T cells using Mission Lentiviral Packaging Mix. Primary $CD4^+$ T cells were transduced using polybrene, stimulated with PHA/IL-2, selected with puromycin, and infected with HIV-1 as described above or alternatively co-cultured with HIV-1-infected MT4 cells.

Statistical Analysis

Statistical tests were performed with GraphPad Prism 5.0 as indicated in the figure legends.

SUPPLEMENTAL INFORMATION

Supplemental Information includes Supplemental Experimental Procedures and five figures and can be found with this article online at http://dx.doi.org/10.1016/j.celrep.2016.09.023.

AUTHOR CONTRIBUTIONS

J.V., F.R., and B.V. conceived and designed the experiments. J.V., F.R., R.R., A.V.N., H.V., and E.N. performed the experiments. J.V., F.R., and B.V. analyzed the data. D.S., D.H., A.V.N., V.I., A.L., W.W., A.B., and F.K. contributed reagents/materials/analysis protocols and tools. J.V. and B.V. wrote the paper. All authors read and approved the final manuscript.

ACKNOWLEDGMENTS

We thank the Programme EVA Centre for AIDS Reagents, NIBSC (UK) and Dr. Q. Sattentau for providing Jurkat CD4 CCR5 and HL-116 cells, respectively; Dr. K. Fransen for the MT4 cells; Dr. O. Fackler for STING-expressing TZM-bl cells; and Dr. K. Arien for HIV-1 VI203 (D2) and HIV-2 CI85 isolates. The following reagents were obtained through the AIDS Research and Reference Reagent Program, NIH: nevirapine; raltegravir; ritonavir; HIV-1 92UG029 (A8) from the UNAIDS Network for HIV Isolation and Characterization; and pNL4-3 from Dr. M. Martin. We would also like to acknowledge Dr. D.N. Levy, Dr. M.J. Tremblay, Dr. Z. Debyser, Dr. N. Manel, and Dr. F. Margottin-Goguet for the kind donation of HIV constructs as indicated in the table in the Supplemental Experimental Procedures. We also like to thank Dr. N. Manel for the kind gift of pCMV-ΔR8.91 and the pLKO.1-puro-shIRF3 vector and Dr. J. Van Damme for the kind gift of goat anti-human IFN-β serum. Dr. O. Schwartz is acknowledged for his continuous support and contribution of reagents and Cristina Garcia Timermans for technical assistance.

This work was supported by an SBO CellCoVir grant from the agency for Innovation by Science and Technology (IWT) (Flanders, Belgium); the HIV-STOP Interuniversity Attraction Poles program of Belgian Science Policy; the European Union FP7 Health-2007-2.3.2-1 Collaborative Project iNEF; Ghent University grant BOF11/GOA/013; HIVERA IRIFCURE; and grants from the Research Foundation Flanders (FWO) to B.V. J.V., A.L., and W.W. are PhD fellows, and B.V. is a Senior Clinical Investigator of the FWO. V.I. was supported by the BOF program Ghent University. F.R. and R.R. are PhD fellows of Université Denis Diderot and were supported by grants from ANRS, SIDACTION, AREVA Foundation, FP7 program "HIT HIDDEN HIV" (Health-F3-2012-305762), the Vaccine Research Institute (ANR-10-LABX-77), and Institut Pasteur. D.S. and D.H. were supported by the International Graduate School in Molecular Medicine, Ulm. F.K. was supported by the Deutsche Forschungsgemeinschaft, FP7 "HIT HIDDEN HIV," and an ERC advanced grant (Anti-Virome). The funders had no role in study design, data collection and analysis, the decision to publish, or preparation of the manuscript.

Received: May 13, 2015
Revised: July 18, 2016
Accepted: September 8, 2016
Published: October 4, 2016

REFERENCES

Abe, T., and Barber, G.N. (2014). Cytosolic-DNA-mediated, STING-dependent proinflammatory gene induction necessitates canonical NF-κB activation through TBK1. J. Virol. *88*, 5328–5341.

Arien, K.K., Abraha, A., Quinones-Mateu, M.E., Kestens, L., Vanham, G., and Arts, E.J. (2005). The replicative fitness of primary human immunodeficiency virus type 1 (HIV-1) group M, HIV-1 group O, and HIV-2 isolates. J Virol. *79*, 8979–8990.

Besnard-Guerin, C., Belaïdouni, N., Lassot, I., Segeral, E., Jobart, A., Marchal, C., and Benarous, R. (2004). HIV-1 Vpu sequesters beta-transducin repeat-containing protein (betaTrCP) in the cytoplasm and provokes the accumulation of beta-catenin and other SCFbetaTrCP substrates. J. Biol. Chem. *279*, 788–795.

Bour, S., Perrin, C., Akari, H., and Strebel, K. (2001). The human immunodeficiency virus type 1 Vpu protein inhibits NF-kappa B activation by interfering with beta TrCP-mediated degradation of Ikappa B. J. Biol. Chem. *276*, 15920–15928.

Casey, L., Wen, X., and de Noronha, C.M. (2010). The functions of the HIV1 protein Vpr and its action through the DCAF1.DDB1.Cullin4 ubiquitin ligase. Cytokine *51*, 1–9.

Chatzinikolaou, G., Karakasilioti, I., and Garinis, G.A. (2014). DNA damage and innate immunity: links and trade-offs. Trends Immunol. *35*, 429–435.

DeHart, J.L., Zimmerman, E.S., Ardon, O., Monteiro-Filho, C.M., Argañaraz, E.R., and Planelles, V. (2007). HIV-1 Vpr activates the G2 checkpoint through manipulation of the ubiquitin proteasome system. Virol. J. *4*, 57.

Del Portillo, A., Tripodi, J., Najfeld, V., Wodarz, D., Levy, D.N., and Chen, B.K. (2011). Multiploid inheritance of HIV-1 during cell-to-cell infection. J. Virol. *85*, 7169–7176.

Doehle, B.P., Hladik, F., McNevin, J.P., McElrath, M.J., and Gale, M., Jr. (2009). Human immunodeficiency virus type 1 mediates global disruption of innate antiviral signaling and immune defenses within infected cells. J. Virol. *83*, 10395–10405.

Doehle, B.P., Chang, K., Fleming, L., McNevin, J., Hladik, F., McElrath, M.J., and Gale, M., Jr. (2012). Vpu-deficient HIV strains stimulate innate immune signaling responses in target cells. J. Virol. *86*, 8499–8506.

Doitsh, G., Galloway, N.L., Geng, X., Yang, Z., Monroe, K.M., Zepeda, O., Hunt, P.W., Hatano, H., Sowinski, S., Muñoz-Arias, I., and Greene, W.C. (2014). Cell death by pyroptosis drives CD4 T-cell depletion in HIV-1 infection. Nature *505*, 509–514.

Engelman, A., Englund, G., Orenstein, J.M., Martin, M.A., and Craigie, R. (1995). Multiple effects of mutations in human immunodeficiency virus type 1 integrase on viral replication. J. Virol. *69*, 2729–2736.

Galão, R.P., Le Tortorec, A., Pickering, S., Kueck, T., and Neil, S.J. (2012). Innate sensing of HIV-1 assembly by Tetherin induces NFκB-dependent proinflammatory responses. Cell Host Microbe *12*, 633–644.

Gao, D., Wu, J., Wu, Y.T., Du, F., Aroh, C., Yan, N., Sun, L., and Chen, Z.J. (2013). Cyclic GMP-AMP synthase is an innate immune sensor of HIV and other retroviruses. Science *341*, 903–906.

Gratton, S., Cheynier, R., Dumaurier, M.J., Oksenhendler, E., and Wain-Hobson, S. (2000). Highly restricted spread of HIV-1 and multiply infected cells within splenic germinal centers. Proc. Natl. Acad. Sci. USA *97*, 14566–14571.

Hardy, G.A., Sieg, S., Rodriguez, B., Anthony, D., Asaad, R., Jiang, W., Mudd, J., Schacker, T., Funderburg, N.T., Pilch-Cooper, H.A., et al. (2013). Interferon-α is the primary plasma type-I IFN in HIV-1 infection and correlates with immune activation and disease markers. PLoS ONE *8*, e56527.

Harman, A.N., Lai, J., Turville, S., Samarajiwa, S., Gray, L., Marsden, V., Mercier, S.K., Jones, K., Nasr, N., Rustagi, A., et al. (2011). HIV infection of dendritic cells subverts the IFN induction pathway via IRF-1 and inhibits type 1 IFN production. Blood *118*, 298–308.

Hotter, D., Kirchhoff, F., and Sauter, D. (2013). HIV-1 Vpu does not degrade interferon regulatory factor 3. J. Virol. *87*, 7160–7165.

Huang, C.Y., Chiang, S.F., Lin, T.Y., Chiou, S.H., and Chow, K.C. (2012). HIV-1 Vpr triggers mitochondrial destruction by impairing Mfn2-mediated ER-mitochondria interaction. PLoS ONE *7*, e33657.

Imbeault, M., Ouellet, M., and Tremblay, M.J. (2009). Microarray study reveals that HIV-1 induces rapid type-I interferon-dependent p53 mRNA up-regulation in human primary CD4+ T cells. Retrovirology *6*, 5.

Jacotot, E., Ferri, K.F., El Hamel, C., Brenner, C., Druillennec, S., Hoebeke, J., Rustin, P., Métivier, D., Lenoir, C., Geuskens, M., et al. (2001). Control of mitochondrial membrane permeabilization by adenine nucleotide translocator interacting with HIV-1 viral protein rR and Bcl-2. J. Exp. Med. *193*, 509–519.

Jakobsen, M.R., Bak, R.O., Andersen, A., Berg, R.K., Jensen, S.B., Tengchuan, J., Laustsen, A., Hansen, K., Ostergaard, L., Fitzgerald, K.A., et al. (2013). IFI16 senses DNA forms of the lentiviral replication cycle and controls HIV-1 replication. Proc. Natl. Acad. Sci. USA *110*, E4571–E4580.

Jung, A., Maier, R., Vartanian, J.P., Bocharov, G., Jung, V., Fischer, U., Meese, E., Wain-Hobson, S., and Meyerhans, A. (2002). Recombination: Multiply infected spleen cells in HIV patients. Nature *418*, 144.

Kader, M., Smith, A.P., Guiducci, C., Wonderlich, E.R., Normolle, D., Watkins, S.C., Barrat, F.J., and Barratt-Boyes, S.M. (2013). Blocking TLR7- and TLR9-mediated IFN-α production by plasmacytoid dendritic cells does not diminish immune activation in early SIV infection. PLoS Pathog. *9*, e1003530.

Kato, K., Ishii, R., Goto, E., Ishitani, R., Tokunaga, F., and Nureki, O. (2013). Structural and functional analyses of DNA-sensing and immune activation by human cGAS. PLoS ONE *8*, e76983.

Laguette, N., Brégnard, C., Hue, P., Basbous, J., Yatim, A., Larroque, M., Kirchhoff, F., Constantinou, A., Sobhian, B., and Benkirane, M. (2014). Premature activation of the SLX4 complex by Vpr promotes G2/M arrest and escape from innate immune sensing. Cell *156*, 134–145.

Lahaye, X., Satoh, T., Gentili, M., Cerboni, S., Conrad, C., Hurbain, I., El Marjou, A., Lacabaratz, C., Lelièvre, J.D., and Manel, N. (2013). The capsids of HIV-1 and HIV-2 determine immune detection of the viral cDNA by the innate sensor cGAS in dendritic cells. Immunity *39*, 1132–1142.

Lepelley, A., Louis, S., Sourisseau, M., Law, H.K., Pothlichet, J., Schilte, C., Chaperot, L., Plumas, J., Randall, R.E., Si-Tahar, M., et al. (2011). Innate sensing of HIV-infected cells. PLoS Pathog. *7*, e1001284.

Liu, R., Lin, Y., Jia, R., Geng, Y., Liang, C., Tan, J., and Qiao, W. (2014). HIV-1 Vpr stimulates NF-κB and AP-1 signaling by activating TAK1. Retrovirology *11*, 45.

Louwagie, J., McCutchan, F.E., Peeters, M., Brennan, T.P., Sanders-Buell, E., Eddy, G.A., van der Groen, G., Fransen, K., Gershy-Damet, G.M., Deleys, R., et al. (1993). Phylogenetic analysis of gag genes from 70 international HIV-1 isolates provides evidence for multiple genotypes. AIDS *7*, 769–780.

Lum, J.J., Cohen, O.J., Nie, Z., Weaver, J.G., Gomez, T.S., Yao, X.J., Lynch, D., Pilon, A.A., Hawley, N., Kim, J.E., et al. (2003). Vpr R77Q is associated with long-term nonprogressive HIV infection and impaired induction of apoptosis. J. Clin. Invest. *111*, 1547–1554.

Manel, N., Hogstad, B., Wang, Y., Levy, D.E., Unutmaz, D., and Littman, D.R. (2010). A cryptic sensor for HIV-1 activates antiviral innate immunity in dendritic cells. Nature *467*, 214–217.

Manganaro, L., de Castro, E., Maestre, A.M., Olivieri, K., García-Sastre, A., Fernandez-Sesma, A., and Simon, V. (2015). HIV Vpu interferes with NF-κB activity but not with interferon regulatory factor 3. J. Virol. *89*, 9781–9790.

Martin-Gayo, E., Buzon, M.J., Ouyang, Z., Hickman, T., Cronin, J., Pimenova, D., Walker, B.D., Lichterfeld, M., and Yu, X.G. (2015). Potent cell-intrinsic immune responses in dendritic cells facilitate HIV-1-specific T cell immunity in HIV-1 elite controllers. PLoS Pathog. *11*, e1004930.

Mashiba, M., Collins, D.R., Terry, V.H., and Collins, K.L. (2014). Vpr overcomes macrophage-specific restriction of HIV-1 Env expression and virion production. Cell Host Microbe *16*, 722–735.

Merindol, N., and Berthoux, L. (2015). Restriction factors in HIV-1 disease progression. Curr. HIV Res. *13*, 448–461.

Monroe, K.M., Yang, Z., Johnson, J.R., Geng, X., Doitsh, G., Krogan, N.J., and Greene, W.C. (2014). IFI16 DNA sensor is required for death of lymphoid CD4 T cells abortively infected with HIV. Science *343*, 428–432.

Nascimbeni, M., Perié, L., Chorro, L., Diocou, S., Kreitmann, L., Louis, S., Garderet, L., Fabiani, B., Berger, A., Schmitz, J., et al. (2009). Plasmacytoid dendritic cells accumulate in spleens from chronically HIV-infected patients but barely participate in interferon-alpha expression. Blood *113*, 6112–6119.

Nasr, N., Maddocks, S., Turville, S.G., Harman, A.N., Woolger, N., Helbig, K.J., Wilkinson, J., Bye, C.R., Wright, T.K., Rambukwelle, D., et al. (2012). HIV-1 infection of human macrophages directly induces viperin which inhibits viral production. Blood *120*, 778–788.

Okumura, A., Alce, T., Lubyova, B., Ezelle, H., Strebel, K., and Pitha, P.M. (2008). HIV-1 accessory proteins VPR and Vif modulate antiviral response by targeting IRF-3 for degradation. Virology *373*, 85–97.

Pickering, S., Hué, S., Kim, E.Y., Reddy, S., Wolinsky, S.M., and Neil, S.J. (2014). Preservation of tetherin and CD4 counter-activities in circulating Vpu alleles despite extensive sequence variation within HIV-1 infected individuals. PLoS Pathog. *10*, e1003895.

Puigdomènech, I., Casartelli, N., Porrot, F., and Schwartz, O. (2013). SAMHD1 restricts HIV-1 cell-to-cell transmission and limits immune detection in monocyte-derived dendritic cells. J. Virol. *87*, 2846–2856.

Rasaiyaah, J., Tan, C.P., Fletcher, A.J., Price, A.J., Blondeau, C., Hilditch, L., Jacques, D.A., Selwood, D.L., James, L.C., Noursadeghi, M., and Towers, G.J. (2013). HIV-1 evades innate immune recognition through specific cofactor recruitment. Nature *503*, 402–405.

Roesch, F., Richard, L., Rua, R., Porrot, F., Casartelli, N., and Schwartz, O. (2015). Vpr enhances tumor necrosis factor production by HIV-1-infected T cells. J. Virol. *89*, 12118–12130.

Roux, P., Alfieri, C., Hrimech, M., Cohen, E.A., and Tanner, J.E. (2000). Activation of transcription factors NF-kappaB and NF-IL-6 by human immunodeficiency virus type 1 protein R (Vpr) induces interleukin-8 expression. J. Virol. *74*, 4658–4665.

Sandler, N.G., Bosinger, S.E., Estes, J.D., Zhu, R.T., Tharp, G.K., Boritz, E., Levin, D., Wijeyesinghe, S., Makamdop, K.N., del Prete, G.Q., et al. (2014). Type I interferon responses in rhesus macaques prevent SIV infection and slow disease progression. Nature *511*, 601–605.

Sauter, D., Schindler, M., Specht, A., Landford, W.N., Münch, J., Kim, K.A., Votteler, J., Schubert, U., Bibollet-Ruche, F., Keele, B.F., et al. (2009). Tetherin-driven adaptation of Vpu and Nef function and the evolution of pandemic and nonpandemic HIV-1 strains. Cell Host Microbe *6*, 409–421.

Sauter, D., Hotter, D., Van Driessche, B., Stürzel, C.M., Kluge, S.F., Wildum, S., Yu, H., Baumann, B., Wirth, T., Plantier, J.C., et al. (2015). Differential regulation of NF-κB-mediated proviral and antiviral host gene expression by primate lentiviral Nef and Vpu proteins. Cell Rep. *10*, 586–599.

Schoggins, J.W., MacDuff, D.A., Imanaka, N., Gainey, M.D., Shrestha, B., Eitson, J.L., Mar, K.B., Richardson, R.B., Ratushny, A.V., Litvak, V., et al. (2014). Pan-viral specificity of IFN-induced genes reveals new roles for cGAS in innate immunity. Nature *505*, 691–695.

Sigal, A., Kim, J.T., Balazs, A.B., Dekel, E., Mayo, A., Milo, R., and Baltimore, D. (2011). Cell-to-cell spread of HIV permits ongoing replication despite antiretroviral therapy. Nature *477*, 95–98.

Sivro, A., Su, R.C., Plummer, F.A., and Ball, T.B. (2014). Interferon responses in HIV infection: from protection to disease. AIDS Rev. *16*, 43–51.

Sourisseau, M., Sol-Foulon, N., Porrot, F., Blanchet, F., and Schwartz, O. (2007). Inefficient human immunodeficiency virus replication in mobile lymphocytes. J. Virol. *81*, 1000–1012.

Trotard, M., Tsopoulidis, N., Tibroni, N., Willemsen, J., Binder, M., Ruggieri, A., and Fackler, O.T. (2015). Sensing of HIV-1 infection in Tzm-bl cells with reconstituted expression of STING. J. Virol. *90*, 2064–2076.

West, A.P., Khoury-Hanold, W., Staron, M., Tal, M.C., Pineda, C.M., Lang, S.M., Bestwick, M., Duguay, B.A., Raimundo, N., MacDuff, D.A., et al. (2015). Mitochondrial DNA stress primes the antiviral innate immune response. Nature *520*, 553–557.

Yan, N., Regalado-Magdos, A.D., Stiggelbout, B., Lee-Kirsch, M.A., and Lieberman, J. (2010). The cytosolic exonuclease TREX1 inhibits the innate immune response to human immunodeficiency virus type 1. Nat. Immunol. *11*, 1005–1013.

Yoh, S.M., Schneider, M., Seifried, J., Soonthornvacharin, S., Akleh, R.E., Olivieri, K.C., De Jesus, P.D., Ruan, C., de Castro, E., Ruiz, P.A., et al. (2015). PQBP1 is a proximal sensor of the cGAS-dependent innate response to HIV-1. Cell *161*, 1293–1305.

Zahoor, M.A., Xue, G., Sato, H., Murakami, T., Takeshima, S.N., and Aida, Y. (2014). HIV-1 Vpr induces interferon-stimulated genes in human monocyte-derived macrophages. PLoS ONE *9*, e106418.

Zahoor, M.A., Xue, G., Sato, H., and Aida, Y. (2015). Genome-wide transcriptional profiling reveals that HIV-1 Vpr differentially regulates interferon-stimulated genes in human monocyte-derived dendritic cells. Virus Res. *208*, 156–163.

Cell Reports, Volume *17*

Supplemental Information

HIV Triggers a cGAS-Dependent, Vpu- and Vpr-Regulated Type I Interferon Response in CD4$^+$ T Cells

Jolien Vermeire, Ferdinand Roesch, Daniel Sauter, Réjane Rua, Dominik Hotter, Anouk Van Nuffel, Hanne Vanderstraeten, Evelien Naessens, Veronica Iannucci, Alessia Landi, Wojciech Witkowski, Ann Baeyens, Frank Kirchhoff, and Bruno Verhasselt

Supplemental Data

Figure S1

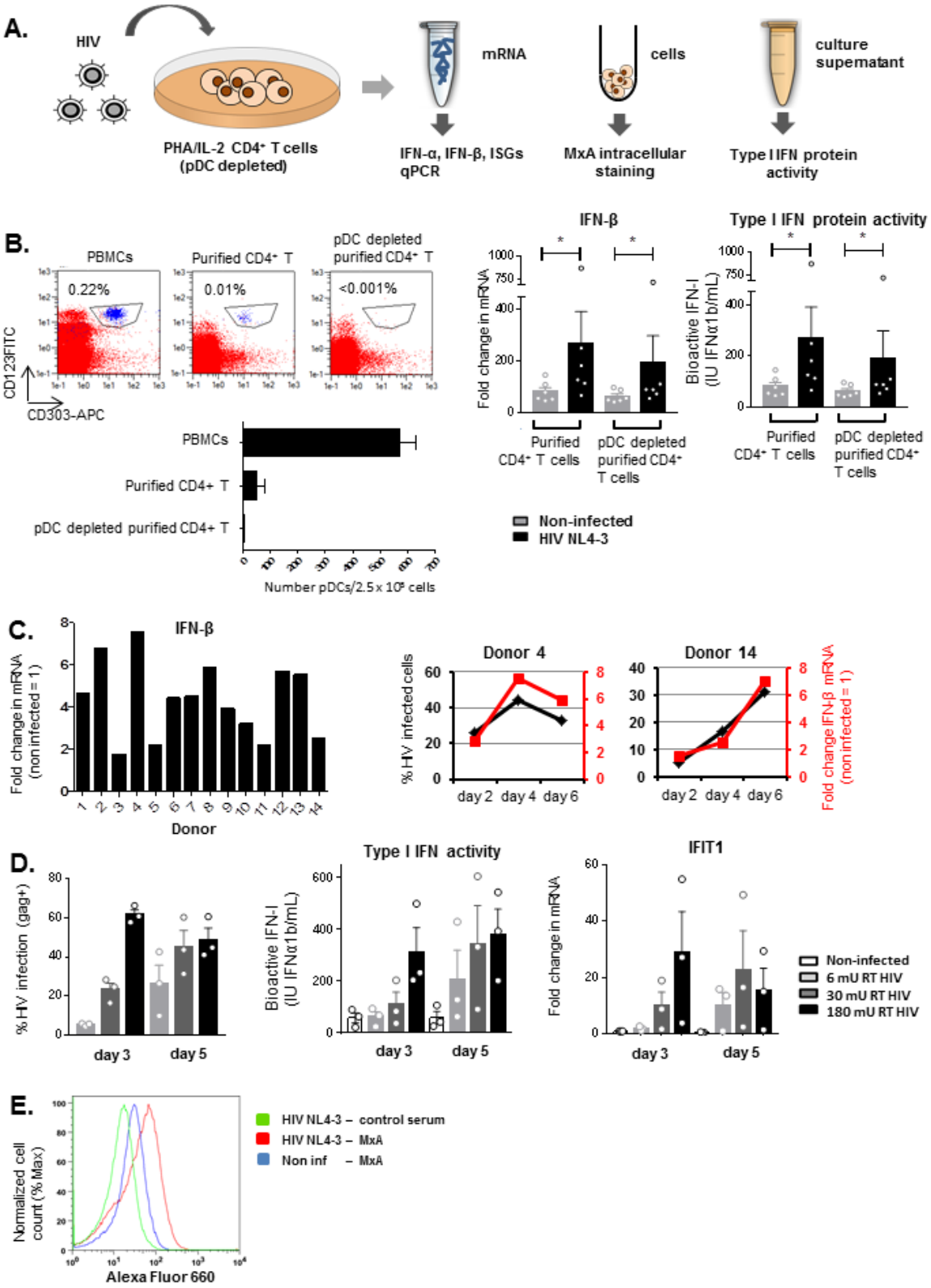

Figure S1, related to Figure 1.
Characterization of IFN-I response during HIV infection primary CD4$^+$ T cells.
(A) Experimental scheme to measure type 1 IFN (IFN-I) response: PHA/IL-2 activated, pDC depleted primary CD4$^+$ T cells are infected with HIV. The IFN-I response is quantified by isolation of mRNA from the cells to measure IFN-α, IFN-β and IFN-stimulated gene (ISGs) expression by qPCR, by intracellular staining of the cells for MxA protein and by measuring IFN-I activity in the supernatant of the cells with the HL-116 reporter cell assay.
(B) (Left) Dot-plots of flow cytometric data showing expression of pDC markers (CD123-FITC versus CD303-APC) in PBMCs and purified CD4$^+$ T cell populations with or without additional pDC depletion, immediately after isolation of cells in a representative experiment. Red dots represent cells gated on viable (propidium iodide-negative) cells, blue represents cells with additional gating on CD304+CD123+ cells. Numbers indicate the percentage of CD304+CD123+CD303+ cells among viable cells. Graph shows average number of CD304+CD123+CD303+ cells per 250,000 cells detected as described above (n=6). Purified CD4$^+$ T cells populations typically contained around 20 pDC's per culture of 250,000 cells, while CD4$^+$ T cells with additional pDC depletion contained ≤ 1 pDC per culture.
(Middle) Fold change in IFN-β mRNA levels relative to non-infected cells and (left) IFN-I activity for purified CD4$^+$ T cells with or without additional pDC depletion at peak levels of HIV NL4-3-GFP-I or HIV NL4-3-HSA-I infection (4 or 6 days after infection) (n=6).
(C) (Left) Fold change in IFN-β mRNA levels relative to non-infected cells, 4 days after HIV NL4-3-GFP-I or HIV NL4-3-HSA-I infection of primary CD4$^+$ T cells derived from 14 different donors; (right) percentage of HIV infected cells (left y-axis) and fold change in IFN-β mRNA levels relative to non-infected cells (right y-axis) at different time points after infection in cells of two of these donors.
(D) Infection levels and IFN-I response in primary CD4$^+$ T cells infected with the indicated amounts of HIV NL4-3 virus (mU RT activity) (n=3). (Left) Percentage of infected cells at different time points after infection, measured by intracellular p24 staining; (middle) IFN-I activity in supernatant of cells; (right) fold change in *IFIT1* mRNA levels at different time points after infection, relative to non-infected cells at day 3.
(E) Histograms showing expression of MxA in HIV NL4-3 infected or non-infected cells primary CD4$^+$ T cells after intracellular staining with a rabbit polyclonal anti-MxA antibody or rabbit control serum, 3 days after infection. Ratio of mean fluorescence intensity of MxA stained over control stained infected cells: 3.
Graphs in **(B)** and **(D)** show data and mean ± SEM. *$p<0.05$ (Wilcoxon matched pairs test).

Figure S2

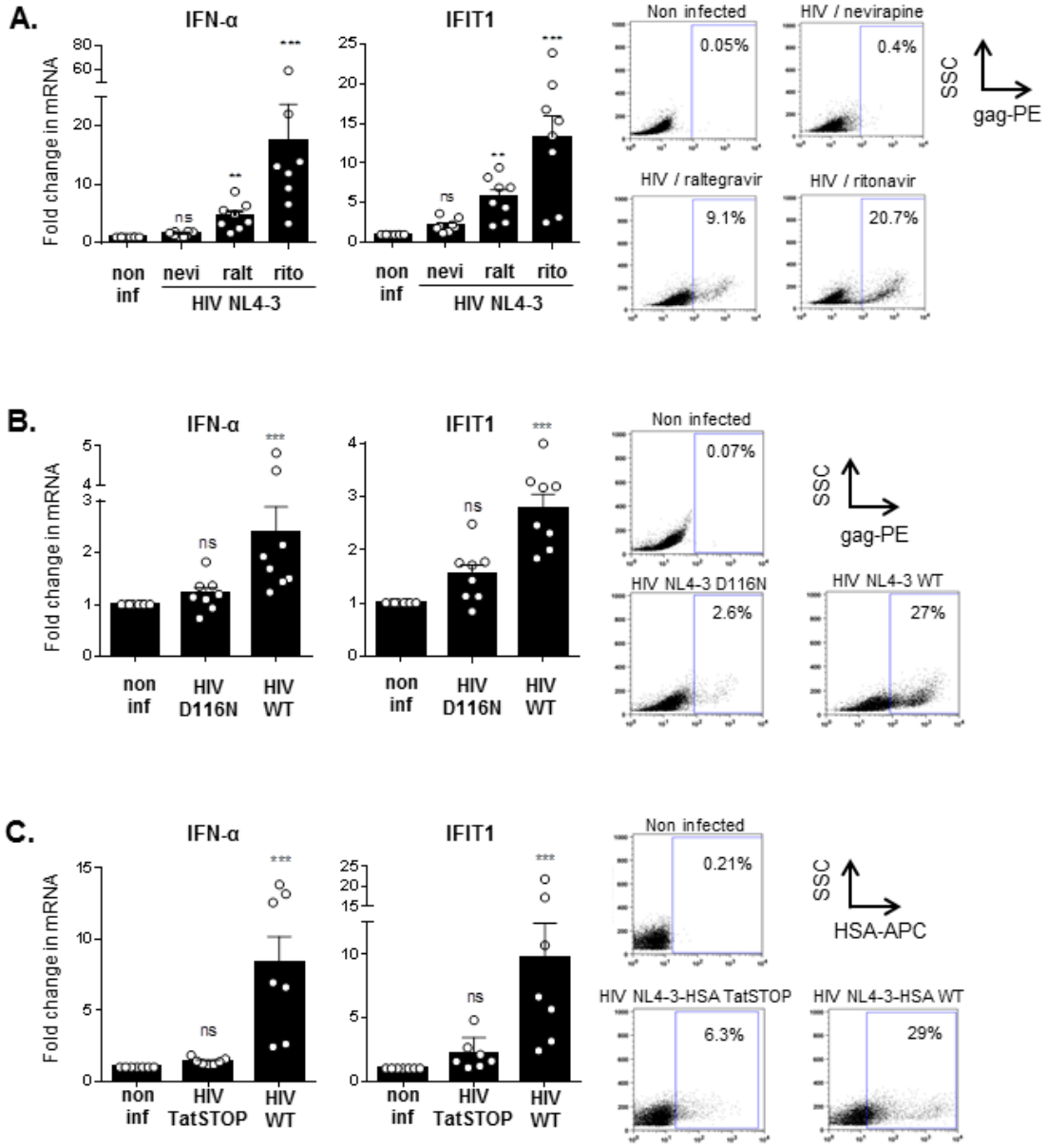
A.
IFN-α
IFIT1
Fold change in mRNA
non inf
nevi
ralt
rito
HIV NL4-3
Non infected
0.05%
HIV / nevirapine
0.4%
HIV / raltegravir
9.1%
HIV / ritonavir
20.7%
SSC
gag-PE
B.
IFN-α
IFIT1
Fold change in mRNA
non inf
HIV D116N
HIV WT
Non infected
0.07%
HIV NL4-3 D116N
2.6%
HIV NL4-3 WT
27%
SSC
gag-PE
C.
IFN-α
IFIT1
Fold change in mRNA
non inf
HIV TatSTOP
HIV WT
Non infected
0.21%
HIV NL4-3-HSA TatSTOP
6.3%
HIV NL4-3-HSA WT
29%
SSC
HSA-APC

Figure S2, related to Figure 3.
Requirement of HIV-1 integration and Tat-mediated viral gene expression for IFN-I induction in primary CD4$^+$ T cells.
(Left) Fold change in IFN-α and *IFIT1* mRNA in infected relative to non-infected (non inf) cells from different donors; (right) dot-plots of flow cytometric data showing side scatter (SSC) versus p24-PE **(A, B)** or HSA-APC **(C)** fluorescent intensity levels measured at the same time point in primary CD4$^+$ T cells infected with:
(A) HIV NL4-3 in the presence of a reverse transcription inhibitor (nevirapine, nevi), integration inhibitor (raltegravir, ralt) or protease inhibitor (ritonavir, rito) 48 h after infection (n=8).
(B) HIV NL4-3 wild-type (HIV WT) or D116N integrase mutant (HIV D116N) 24 h after infection (n=8).
(C) HIV NL4-3-HSA-I wild-type (HIV WT) or *tat*-defective virus (HIV TatStop) in the presence of ritonavir 48 h after infection (n=7).
Graphs show data and mean ± SEM.” ns” not significant, **p<0.01; ***p<0.001 (Friedman test followed by Dunn's multiple comparisons post hoc test, infected compared to non-infected control).

Figure S3

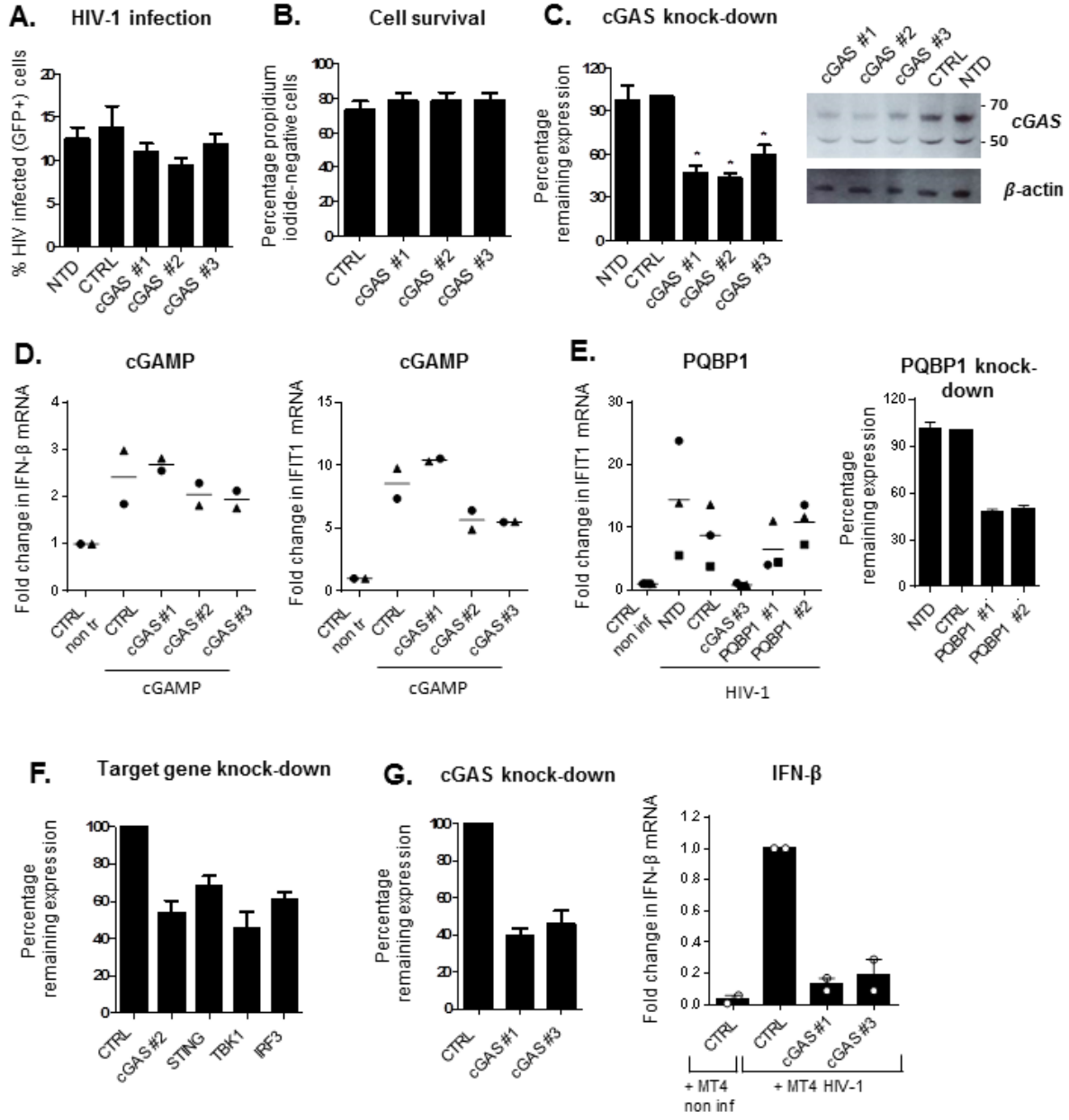
A.
HIV-1 infection
% HIV infected (GFP+) cells
NTD
CTRL
cGAS #1
cGAS #2
cGAS #3
B.
Cell survival
Percentage propidium iodide-negative cells
C.
cGAS knock-down
Percentage remaining expression
cGAS
β-actin
70
50
D.
cGAMP
Fold change in IFN-β mRNA
Fold change in IFIT1 mRNA
CTRL non tr
cGAMP
E.
PQBP1
PQBP1 knock-down
Fold change in IFIT1 mRNA
Percentage remaining expression
CTRL non inf
POBP1 #1
POBP1 #2
HIV-1
F.
Target gene knock-down
STING
TBK1
IRF3
G.
cGAS knock-down
IFN-β
+ MT4 non inf
+ MT4 HIV-1

Figure S3, related to Figure 4.
cGAS is required for IFN-I induction by HIV-1 in primary CD4$^+$ T cells.
(**A**) Percentage of GFP+ (HIV-1 infected) cells in cultures described in Figure 4B (n=6). cGAS #1-3 represents use of different shRNA sequences targeting cGAS; CTRL: cells transduced with a non-targeting shRNA control vector; NTD: non-transduced cells.
(**B**) Percentage of propidium iodide-negative cells as indicated by FACS analysis of transduced cells described in Figure 4B, immediately prior to HIV-1 infection (n=6).
(**C**) (Left) Percentage of remaining cGAS mRNA levels in cells described in Figure 4B, relative to levels in cells transduced with a non-targeting shRNA control vector (CTRL) (100%) immediately prior to HIV-1 infection (n=6). (Right) cGAS protein levels (50 and 60 kDa isoforms) and β-actin loading control in lysates of primary CD4$^+$ T cells after transduction with indicated shRNA-encoding lentiviral vectors and puromycin selection.
(**D**) Fold change in IFN-β (left) and *IFIT1* (right) mRNA in cells transduced with indicated shRNA-encoding lentiviral vectors and stimulation with synthetic cGAMP (10 μg/mL) for 24 h, relative to non-treated (non tr) cells. cGAS #1-3 represents different shRNA sequences used to target cGAS; CTRL: cells transduced with a non-targeting shRNA control vector (n=2).
(**E**) (Left) Fold change in *IFIT1* mRNA in cells transduced with indicated shRNA-encoding lentiviral vectors and infected with VSV-G pseudotyped HIV NL4-3-I-EGFP for 48 h, relative to non-infected (non inf) cells. cGAS #3 and PQBP1 #1-2 represents different shRNA sequences used to target cGAS or PQBP1 respectively; CTRL: cells transduced with a non-targeting shRNA control vector. (Right) Percentage of remaining mRNA expression of the indicated genes in non-infected primary CD4$^+$ T cells transduced with shRNA encoding vectors targeting PQBP1, relative to levels in cells transduced with a non-targeting shRNA control vector (100%) (n=3).
(F) Percentage of remaining mRNA of the indicated genes in primary CD4$^+$ T cells transduced with shRNA encoding pLKO.1 vectors targeting the indicated genes, relative to levels in cells transduced with a non-targeting shRNA control vector (100%) immediately prior to co-culture (n=2-4).
(G) (Left) Percentage of remaining cGAS mRNA in primary CD4$^+$ T cells transduced with additional shRNA encoding pLKO.1 vectors targeting cGAS, relative to levels in cells transduced with a non-targeting shRNA control vector (100%) immediately prior to co-culture (n=2). (Right) Fold change in IFN-β mRNA levels in co-cultures of non-infected (non inf) or HIV NL4-3-GFP-I infected MT4 cells with primary CD4$^+$ T cells transduced with shRNA-encoding vectors targeting cGAS or the shRNA control vector (CTRL), relative to levels obtained in co-cultures of CTRL cells and HIV-1 infected MT4 cells (n=2).
Bar graphs in A-C and E, F, G (left), H represent mean ± SEM. Graphs in D, E (left), G (right) show data (data point symbols refer to individual donors) and mean; * $p<0.05$ (Wilcoxon signed-rank test).

Figure S4

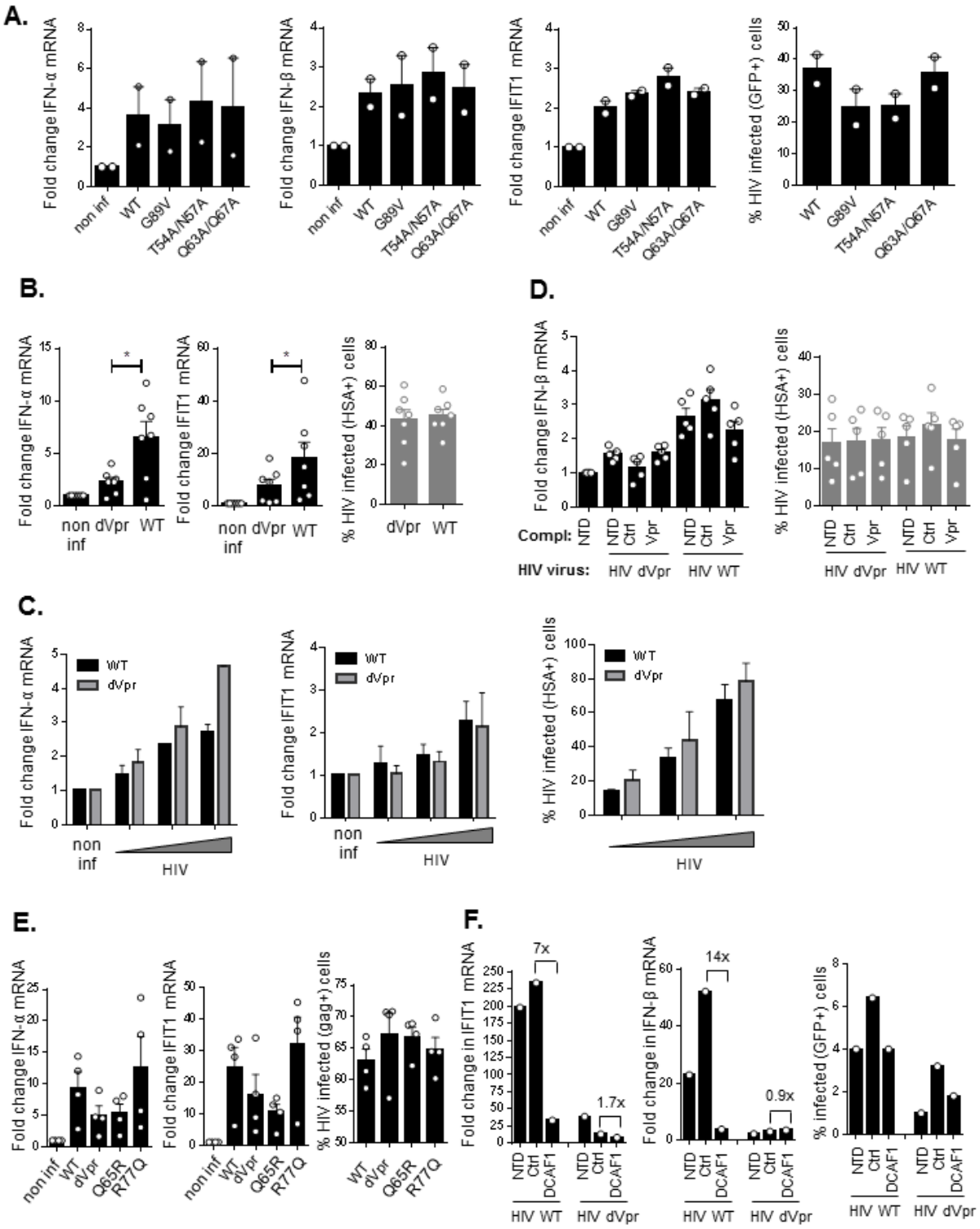
A.
Fold change IFN-α mRNA
Fold change IFN-β mRNA
Fold change IFIT1 mRNA
% HIV infected (GFP+) cells
non inf
WT
G89V
T54A/N57A
Q63A/Q67A
B.
Fold change IFN-α mRNA
Fold change IFIT1 mRNA
% HIV infected (HSA+) cells
non inf
dVpr
WT
D.
Fold change IFN-β mRNA
% HIV infected (HSA+) cells
Compl:
NTD
Ctrl
Vpr
HIV virus:
HIV dVpr
HIV WT
C.
Fold change IFN-α mRNA
Fold change IFIT1 mRNA
% HIV infected (HSA+) cells
WT
dVpr
non inf
HIV
E.
Fold change IFN-α mRNA
Fold change IFIT1 mRNA
% HIV infected (gag+) cells
non inf
WT
dVpr
Q65R
R77Q
F.
Fold change in IFIT1 mRNA
Fold change in IFN-β mRNA
% infected (GFP+) cells
7x
1.7x
14x
0.9x
NTD
Ctrl
DCAF1
HIV WT
HIV dVpr

Figure S4, related to Figure 5.
Effect of HIV-1 Capsid-CypA interaction and Vpr on HIV-1 induced IFN-I response in primary CD4$^+$ T cells.
Infection levels and IFN-I response in primary CD4$^+$ T cells, relative to non-infected (non inf) cells.
(A) Infection with VSV-G pseudotyped HIV-1 LAI dEnv dNef viruses (WT) or with viruses with additional mutations in capsid (G89V, T54A/N57A, Q63A/Q67A), 48 h after infection (n=2). All viruses were complemented with WT capsid during production. (Left to right) Fold change in IFN-α, IFN-β or *IFIT1* mRNA levels; percentage of infected cells (GFP+).
(B) Infection with HIV NL4-3-HSA-I wild-type (WT) or *vpr*-defective virus (dVpr), 48-72 h after infection (n=7). (Left and middle) fold change in IFN-α and *IFIT1* mRNA levels; (right) percentage of infected (HSA+) cells.
(C) Infection of STING expressing TZM-bl cells with increasing concentrations of HIV NL4-3-HSA-I wild-type (WT) or *vpr*-defective virus (dVpr) (1100 to 4400 mU/mL RT activity), 48 h after infection (n=2). (Left and middle) fold change in IFN-α and *IFIT1* mRNA levels relative to non-infected (non inf) cells; (right) percentage of infected (HSA+) cells.
(D) Infection with HIV NL4-3-HSA-I *vpr*-defective (dVpr) or wild-type (WT) virus, not complemented (-), complemented with a control vector (Ctrl) or with WT Vpr (Vpr) during production. Infection was done in the presence of ritonavir (n=5). (Left) Fold change in IFN-β mRNA levels 48 h after infection; (right) percentage of infected (HSA+) cells (n=2).
(E) Infection with HIV NL4-3 viruses: wild-type (WT), *vpr*-deleted (dVpr), viruses with Q65R or R77Q mutation in Vpr, 72 h after infection (n=4). (Left and middle) Fold change in IFN-α and *IFIT1* mRNA; (right) percentage of infected (p24+) cells.
(F) (left) *IFIT1* mRNA levels, (middle) *IFN-β* mRNA levels and (right) percentage of HIV-1 infected cells (GFP+) 48 h after infection with VSV-G pseudotyped HIV NL4-3-I-EGFP wild-type (WT) or *vpr*-deleted (dVpr) virus of cells either not transduced (NTD) or transduced with either a non-targeting control vector (CTRL) or shRNA-encoding lentiviruses targeting DCAF1(n=1). Numbers indicated fold change in *IFIT1* or IFN-β mRNA levels in "CTRL" versus "DCAF1" samples.
Graphs in A, B, D-F show data and mean ± SEM. Graphs in C represent mean ± SEM *$p<0.05$ (Wilcoxon matched pairs test).

Figure S5

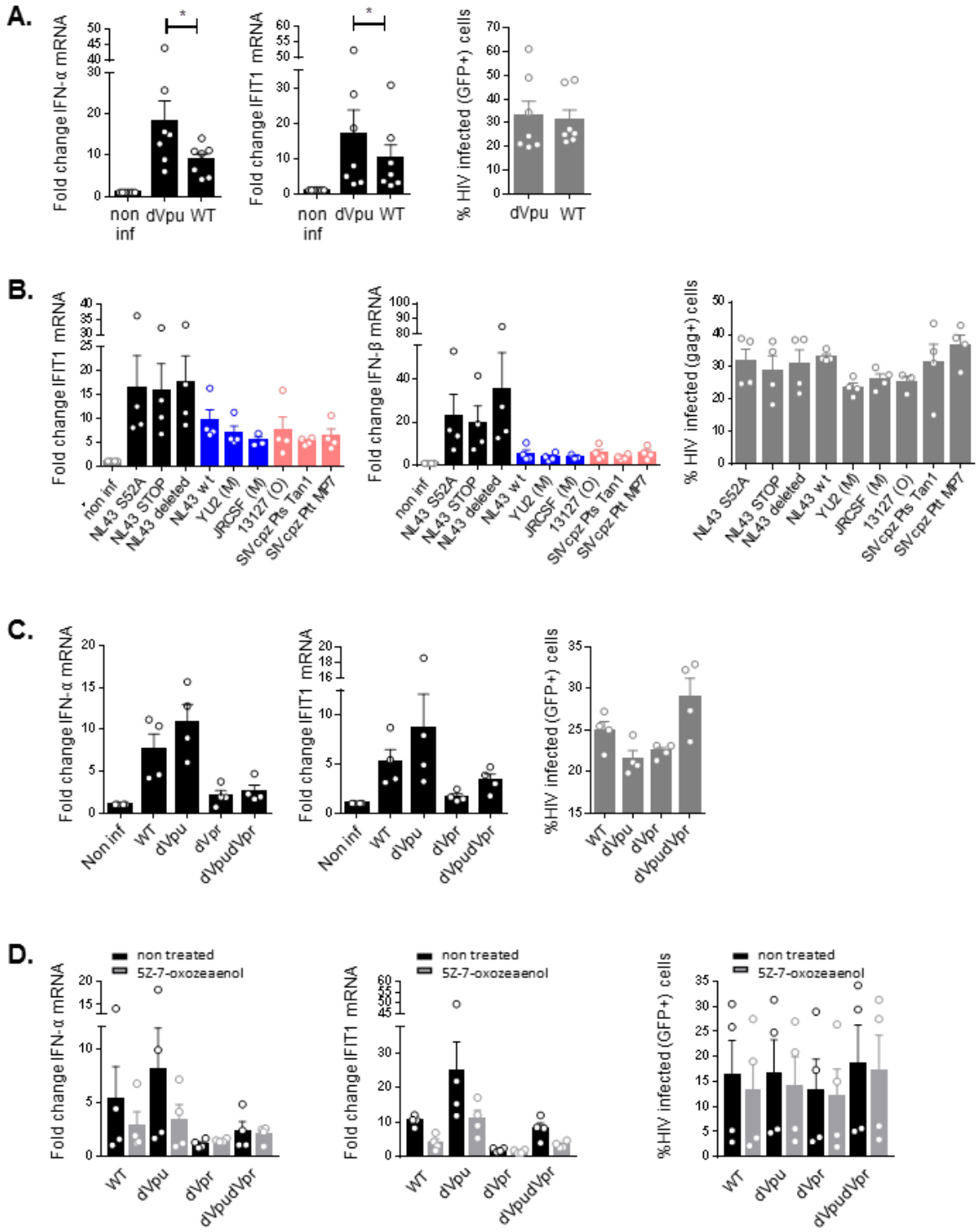
A.
Fold change IFN-α mRNA
Fold change IFIT1 mRNA
% HIV infected (GFP+) cells
non inf
dVpu
WT
B.
Fold change IFIT1 mRNA
Fold change IFN-β mRNA
% HIV infected (gag+) cells
non inf
NL43 S52A
NL43 STOP
NL43 deleted
NL43 wt
YU2 (M)
JRCSF (M)
13127 (O)
SIVcpz Pts Tan1
SIVcpz Ptt MP7
C.
Fold change IFN-α mRNA
Fold change IFIT1 mRNA
%HIV infected (GFP+) cells
Non inf
WT
dVpu
dVpr
dVpudVpr
D.
non treated
5Z-7-oxozeaenol
Fold change IFN-α mRNA
Fold change IFIT1 mRNA
%HIV infected (GFP+) cells
WT
dVpu
dVpr
dVpudVpr

Figure S5, related to Figure 6.
Effect of Vpu on HIV-1 induced IFN-I response in primary CD4$^+$ T cells.
Infection levels and IFN-I response in primary CD4$^+$ T cells, relative to non-infected (non inf) cells.
(A) Infection with VSV-G pseudotyped HIV NL4-3-I-EGFP *vpu*-deleted (dVpu) or wild-type (WT) virus, 48 h after infection (n=7). (Left and middle) fold change in IFN-α and *IFIT1* mRNA levels; (right) percentage of infected (GFP+) cells.
(B) Infection with VSV-G pseudotyped HIV-NL4-3-Vpu-IRES-Env viruses in which the original *vpu* allele was replaced by the *vpu* allele of the indicated HIV-1 or SIV strain. Black bars show viruses with mutated NL4-3 *vpu* alleles, blue bars show viruses with *vpu* alleles that antagonize human tetherin, red bars show viruses with *vpu* alleles that do antagonize human tetherin, 48 h after infection (n=4). (Left and middle) fold change in *IFIT1* and IFN-β mRNA levels; (right) percentage of infected (p24+) cells.
(C) Infection with VSV-G pseudotyped HIV NL4-3-I-EGFP wild-type (WT), *vpu*-deleted (dVpu), *vpr*-deleted (dVpr) or *vpu*- and *vpr*-deleted (dVpu dVpr) viruses, 48 h after infection (n=4). (Left and middle) Fold change in IFN-α and *IFIT1* mRNA levels; (right) percentage of infected (GFP+) cells.
(D) Infection with VSV-G pseudotyped HIV NL4-3-I-EGFP wild-type (WT), *vpu*-deleted (dVpu), *vpr*-deleted (dVpr) or *vpu*- and *vpr*-deleted (dVpu dVpr) viruses, 48 h after infection in presence or absence of 50 nM of TAK1 inhibitor (5Z)-7-oxozeaenol (n=6). (Left and middle) Fold change in IFN-α and *IFIT1* mRNA levels; (right) percentage of infected (GFP+) cells.
Graphs show data and mean ± SEM. *$p<0.05$ (Wilcoxon matched pairs test).

Supplemental Experimental Procedures.

Isolation and culture of cells

Primary $CD4^+$ T cells were isolated from buffy coats of healthy donors (Red Cross, Ghent, Belgium), donated after informed consent, approved by Ghent University ethical committee. Peripheral blood mononuclear cells (PBMCs) were obtained on Lymphoprep (Axis-Shield PoC, Oslo, Norway) and used for $CD4^+$ T cell isolation by negative selection with a commercial kit (Miltenyi Biotec, Bergisch Gladbach, Germany) according to manufacturer's instructions. Depletion of pDCs was done on PBMCs prior to isolation of $CD4^+$ T cells, by negative selection after staining with CD304-PE antibody (clone AD5-17F6, Miltenyi Biotec) in the presence of human FcR blocking reagent (Miltenyi Biotec) and subsequent staining with anti-PE paramagnetic microbeads (Miltenyi Biotec). Purity of the $CD4^+$ T cell population was measured by flow cytometry (MACSquant® Analyzer using MACSQuantify v2.4 software, Miltenyi Biotec), showing a fraction of at least 95 % $CD4^+CD3^+$ double positive cells and less than 0.0004 % $CD123^+CD304^+CD303^+$ cells (measured on 1.5 $x10^6$ cells, corresponds to ≤1 pDC per culture of 250,000 cells). Antibodies used for staining were CD3-PE (clone SK7, Becton Dickinson (BD) Biosciences, Erembodegem, Belgium) and CD4-APC (clone MT4 66, Miltenyi Biotech) or CD123-FITC (clone AC145, Miltenyi Biotech), CD303-APC (clone AC144, Miltenyi Biotech) and CD304-PE. Except when used for lentiviral transduction (see below), primary $CD4^+$ T cells cells were cultured for 3 days after isolation at 37 °C in a 5 % (v/v) CO_2 humidified atmosphere in RPMIc: Gibco® RPMI medium 1640 (Life Technologies, Merelbeke, Belgium) supplemented with 2 mM L-glutamin (Life Technologies), 10 % (v/v) heat-inactivated fetal calf serum (Hyclone, Thermo Fisher Scientific, Waltham, MA), 100 U/mL penicillin and 100 µg/mL streptomycin (Life Technologies). RPMIc was supplemented with 20 ng/mL interleukin-2 (IL-2; specific activity 10 U/ng, Peprotech, London, United Kingdom), and with 1 µg/mL phytohemagglutinin (PHA) mitogen (Thermo Fisher Scientific). Subsequently, cells were infected with HIV.

293T cells (DZSM, Braunschweig, Germany), MT4 cells (kind gift from Dr. Katrien Fransen, Institute of Tropical Medicine, Antwerp, Belgium) used for co-culture with primary $CD4^+$ T cells, TZM-bl cells expressing human STING (kind gift from Dr. Oliver Fackler, University Hospital Heidelberg, Heidelberg, Germany (Trotard et al. 2016)) and Jurkat CD4 CCR5 cells (Programme EVA Centre for AIDS Reagents, NIBSC, UK) were cultured at 37°C in a 7 % (v/v) CO_2 humidified atmosphere, in IMDMc (293T, MT4) or DMEMc (TZM-bl): IMDM or DMEM (Life Technologies) supplemented with 10 % (v/v) fetal bovine serum, 2 mM L-glutamin, 100 U/mL penicillin and 100 µg/mL streptomycin. MT4C5 cells (a derivate MT4 cells expressing CCR5) were used for co-culture with MDDCs and were cultured as described in Lepelley et al. 2011. HL-116 cells (kindly provided by Dr. Uze, University of Montpellier II, France (Uze et al., 1994)) were cultured at 37 °C in a 7 % (v/v) CO_2 humidified atmosphere in DMEM (Life Technologies) supplemented with 10 % fetal bovine serum and 2 mM L-glutamin (DMEMc).

Monocytes were isolated by positive CD14 immunomagnetic selection (Miltenyi Biotec) from PBMCs of healthy donors. MDDCs were generated by culturing monocytes for 5 days in the presence of IL-4 (50 ng/mL) and GM-CSF (10 ng/mL) as described in (Puigdomenech et al., 2013).

Viral constructs

Characteristics and sources of the plasmids used for production of HIV-1 in this study are described in the table below.

HIV-1 encoding vectors used in this study.

Parental vector	**Variant**	**Virus referred to as:**	**Source**	**Reference**
NLENG1-IRES	WT	HIV NL4-3-GFP-I	Dr. D.N. Levy, New York University college of Dentistry, New York, NY	Kutsch et al., 2002; Levy et al., 2004
NL4-3-IRES-HSA	WT	HIV NL4-3-HSA-I	Dr. M.J. Tremblay; Faculté de Médecine, Université Laval, Québec, Canada	Imbeault et al., 2009
	Tat-defective	HIV NL4-3-HSA-I TatSTOP	Constructed in house	See Materials and methods
	Vpr-defective	HIV NL4-3-HSA-I dVpr	Constructed in house	See Materials and methods
pNL4-3	WT	HIV NL4-3	NIH AIDS	Adachi et al., 1986

			Research and Reference Reagent Program	
	Integrase-mutated	HIV NL4-3 D116N	Dr. Z. Debyser, Laboratory for Molecular Virology and Gene Therapy, KU Leuven, Belgium	Mutation introduced in HIV NL4-3 (according to Engelman et al., 1995)
	Vpr-deleted	HIV NL4-3 dVpr	Dr. Margottin-Goguet, Institute Cochin, Paris, France	Le Rouzic et al., 2008
	Vpr Q65R mutant	HIV NL4-3 Q65R	Constructed in house	See Materials and methods
	Vpr R77Q mutant	HIV NL4-3 R77Q	Constructed in house	See Materials and methods
pLaiΔEnv-GFP3	WT	HIV LAI dEnv dNef	Dr. N. Manel, Institut Curie, Paris, France	Manel et al., 2010
	Capsid G89V mutant	HIV LAI dEnv dNef G89V		Manel et al., 2010
	Capsid T54A/N57A mutant	HIV LAI dEnv dNef T54A/N57A		Manel et al., 2010
	Capsid Q63A/Q67A mutant	HIV LAI dEnv dNef Q63A/Q67A		Manel et al., 2010
pBR-NL43-I-EGFP	WT	HIV NL4-3-I-EGFP	Constructed in house	Schindler et al., 2003
	Vpu-deleted	HIV NL4-3-I-EGFP dVpu		Rucker et al., 2004; *nef*-IRES-eGFP introduced as described in Sauter et al., 2009
	Vpr-deleted	HIV NL4-3-I-EGFP dVpr		Rucker et al., 2004; *nef*-IRES-eGFP introduced as described in Sauter et al., 2009
	Vpu-deleted and Vpr-deleted	HIV NL4-3-I-EGFP dVpu dVpr		Rucker et al., 2004; *nef*-IRES-eGFP introduced as described in Sauter et al., 2009
pNL4-3 UIE	WT	HIV NL4-3-Vpu-IRES-Env NL4-3 WT (M)	Constructed in house	Sauter et al., 2009
	Vpu NL4-3 S52 mutant	HIV NL4-3-Vpu-IRES-Env NL4-3 S52		Sauter et al., 2009
	Vpu NL4-3 STOP	HIV NL4-3-Vpu-IRES-Env NL4-3 STOP		Sauter et al., 2009
	Vpu NL4-3 deleted	HIV NL4-3-Vpu-IRES-Env NL4-3 deleted		Sauter et al., 2009
	Vpu HIV-1 M JRCSF	HIV NL4-3-Vpu-IRES-Env JRCSF (M)		Sauter et al., 2009
	Vpu HIV-1 M Yu2 (adapted)	HIV NL4-3-Vpu-IRES-Env Yu2 (M)		Sauter et al., 2009
	Vpu HIV-1 O 13127	HIV NL4-3-Vpu-IRES-Env 13127 (O)		Sauter et al., 2009
	Vpu SIV Cpz Pts	HIV NL4-3-Vpu-		Sauter et al., 2009

	Tan1	IRES-Env Cpz Pts Tan1		
	Vpu SIV Cpz Ptt MP7	HIV NL4-3-Vpu-IRES-Env Cpz Ptt MP7		Sauter et al., 2009

Table shows different HIV-1 constructs used in this study, indicating the parental wild-type (WT) vector and variants used; the name by which this virus is referred to in the study, the source of the vector and the reference describing construction of the vector if published.

The *tat*-defective and *vpr*-defective NL4-3-IRES-HSA vectors were created by site directed mutagenesis on a part of the parental backbone, followed by substitution of the mutated fragment (with verified sequence) in the parental backbone. For mutation of *tat*, a TGA stop codon was introduced after the ATG start codon of the first exon of *tat.* For mutation of *vpr*, the CTAGAGCTTTTAGAGAA sequence at the end of the *vif-vpr* overlapping reading frame, was replaced by a CTAG**TG**AT**TGA**A**TAG**GAA sequence, thereby introducing a stop codon in *vpr* in each of the reading frames after the end of *vif.*
The HIV NL4-3 constructs encoding viruses with Q65R and R77Q mutations in Vpr, were generated by introducing point mutations in HIV NL4-3 WT with the QuikChange XL Site-Directed Mutagenesis kit (Stratagene, Agilent Technologies, La Jolla, CA), using the primers described in table below.

Primers used for mutation of *vpr* in HIV NL4-3 viruses.

Mutation	Forward primer	Reverse Primer
Q65R	5'-agtggaagccataataagaattctgagacaactgctgtttattcattcaga-3'	5'-tctgaaatgaataaacagcagttgtctcagaattcttattatggcttccact-3'
R77Q	5'-gaattatgcctattctgctatgttgacacccaattctgaaatgaata-3'	5'-tattcatttcagaattgggtgtcaacatagcagaataggcataattc-3'

The LZRS-Vpr-IRES-NGFR retroviral vector used for complementation of HIV viruses with a wild-type Vpr protein during production, was constructed by PCR amplification of the *vpr* gene from the NL4-3-IRES-HSA vector and introduction into LZRS-IRES-NGFR (Stove et al., 2005), expressing Nerve Growth Factor Receptor (NGFR) as a marker gene.

Production of HIV

HIV production was done by transfection of 293T cells with Calcium Phosphate Transfection Kit (Life Technologies) or JetPei® (Polyplus, Sélestat, France), according to manufacturer's instructions using 5 µg of HIV plasmid per 750,000 cells. For VSV-G pseudotyped viruses, cells were transfected with 1 µg pMD.G plasmid (Stove et al., 2005) and 4 µg of HIV plasmid. Medium was refreshed 24 h after transfection. Viral supernatant was harvested after 48 h and centrifuged at 900 g for 10 min, to clarify the supernatant from remaining cells. Viral titer was determined by measuring reverse transcriptase activity in the supernatant with the SG-PERT assay (as described in Vermeire et al., 2012). Production of VSV-G pseudotyped HIV NL4-3 WT and dVpr viruses used in context of MDDC experiments was performed as previously described (Puigdomenech et al., 2013).
For production of wild-type and *gag*-mutated VSV-G pseudotyped HIV-1 LAI dEnv dNef viruses complemented with a wild-type capsid protein, 293T cells were transfected with 2.7 µg HIV plasmid, 1.7 µg pCMV-ΔR8.91 (kindly provided by Dr. N. Manel (Manel et al., 2010) and 0.7 µg pMD.G plasmid using JetPei®. Viral supernatant was harvested as indicated above.
For complementation of wild-type and *vpr*-defective HIV NL4-3-HSA-I virions with a wild-type Vpr protein, 293T cells were transfected with 1.7 µg HIV plasmid and 3.3 µg LZRS-Vpr-IRES-NGFR (Vpr complemented) or LZRS-IRES-NGFR (control vector) using JetPei®. Viral supernatant was harvested as indicated above and transfection efficiency was determined at the time of harvesting by surface staining with anti-CD24-APC and anti-NGFR-PE (clone ME20.4, Chromaprobe, Maryland Heights, MO). Percentage of $CD24^{+}NGFR^{+}$ cells was determined by flow cytometry (FACSCalibur, BD Biosciences) and always > 40 %. Efficacy of Vpr complementation using this protocol was previously validated by measurement of Vpr protein levels by Western Blot. In some experiments, supernatants of complemented viruses with low titer were concentrated using PEG-it precipitation of viral particles following manufacturer's instructions (PEG-it™ Viral Precipitation Solution, System Biosciences, Mountain View, CA) and subsequent resuspension in IMDMc in 1/5 of the original volume.
HIV-1 group M A8 isolate (92UG029) (Bachmann et al., 1994) was obtained from the NIH AIDS Research and Reference Reagent Program. The HIV-1 group M D2 (VI203) (Louwagie et al., 1993) and HIV-2 CI85 (Arien et al., 2005) strains were previously isolated from patients attending the AIDS clinic at the Institute of Tropical

Medicine in Antwerp, Belgium, with the approval of the ethical committee after written informed consent. Virus stocks were initially obtained after propagation in short-term cultures of PBMCs as described before (Arien et al., 2005) and subsequently expanded by infection and culture of Jurkat CD4 CCR5 cells. To this end, cells were plated at 5 x 10^5 cells per well of a 12-well flat-bottom plate (BD Biosciences) in 1 mL IMDMc and 1 mL of PBMC-derived viral supernatant was added to the cells (viral titer ranging from 350-1150 mU RT/ mL, equivalent to 35-210 ng p24/mL). Supernatant of the Jurkat CD4 CCR5 cells was collected at peak of infection and centrifuged at 900 g for 10 min, to clarify the supernatant from remaining cells.

Infection with HIV

For HIV infection of primary $CD4^+$ T cells, 250,000 cells were seeded per well in a 96-well flat-bottom plate (BD Biosciences) in RPMIc supplemented with 20 ng/mL IL-2 (final concentration). Depending on the experiment 6-3000 mU RT (equivalent to 1–550 ng p24) of HIV virus was added per well in a final volume of 200 µL, with low concentrations (1-40 ng p24) used for long-term experiments (read-out until day 5-7 after infection) and high concentrations (60-550 ng p24) used for short-term experiments (last read-out at day 1-3 after infection). Cells were subsequently spinoculated at 950 g for 90 min at 32 °C. Medium was refreshed with RPMIc (+ IL-2) immediately after spinoculation and for half of the volume every 2 days during subsequent culture. At the indicated time points after infection, cells were harvested to determine HIV infection levels and remaining cells were lysed in 700 µL QIAZOL (miRNeasy mini kit, QIAGEN, Venlo, The Netherlands) according to manufacturer's instruction. Supernatant of the cells was collected after spinoculation of the cells at 350 g for 10 min at 4 °C. Lysates and supernatants were stored at -80 °C until further use.

For HIV-1 infection in the presence of IFN-α and/or IFN-β neutralizing antibodies, primary $CD4^+$ T cells were resuspended immediately after spinoculation in medium containing 1/100,000x diluted goat anti-human IFN-β serum (925, kindly provided by Dr. Van Damme, Rega Institute, KUL, Belgium (Van Damme et al., 1987)) and/or 6,000 neutralizing units (NU)/ mL rabbit polyclonal anti-human IFN-α antibody (PBL Assay Science, Piscataway, NJ). Every 2 days, new medium with antibodies was added to the cells. Neutralizing capacity of the antibodies was verified by incubating them with recombinant IFNα1b or IFNβ1a (Immunotools, Friesoythe, Germany) and evaluating remaining IFN-I activity with the HL-116 assay.

For HIV-1 infection in the presence of antiretrovirals, primary $CD4^+$ T cells were plated in medium with 5 µM nevirapine, 0.5 µM raltegravir or 1 µM ritonavir (AIDS Research and Reference Reagent Program, Division of AIDS, NIAID, NIH, Germantown, MD) 1 h before infection and antiretrovirals were maintained at these concentrations during infection. Antiretrovirals were titrated on primary CD4+ T cells prior to use to verify inhibition of HIV NL4-3-GFP-I replication.

For HIV-1 infection in the presence of a TAK1 inhibitor, primary $CD4^+$ T cells were plated in medium with 50 nM (5Z)-7-oxozeaenol (Tocris Bioscience, Bristol, UK) immediately before infection and inhibitor was maintained at this concentration during infection.

MT4 cells were infected with HIV NL4-3-GFP-I viruses by plating 1.5 x 10^6 cells per well of a 6-well flat-bottom plate (BD Biosciences) and addition of 165-350 mU RT (equivalent to 30-60 ng p24) of virus in a total volume of 6 mL IMDMc. Cells were subsequently spinoculated at 950 g for 90 min at 32 °C. 48 h-72 h after infection, cells were collected and used for co-culture with primary $CD4^+$ T cells.

STING expressing TZM-bl cells were infected with HIV NL4-3-HSA-I viruses by plating 60,000 cells per well of a 12-well flat bottom plate (BD Biosciences) one day beforof and addition of 1100-4400 mU RT (equivalent to 200-800 ng p24) of virus in a total volume of 4.2 mL DMEMc. Cells were subsequently spinoculated at 950 g for 90 min at 32 °C. 48h after infection, cells were harvested to determine HIV infection levels and remaining cells were lysed in 700 µL QIAZOL (miRNeasy mini kit, QIAGEN, Venlo, The Netherlands) according to manufacturer's instruction.

For infection of MDDCs, 8 x 10^4 MDDCs were seeded in flat-bottomed 96-well plates. MT4C5 cells were infected with VSV-G pseudotyped HIV NL4-3 WT or dVpr, 24-48 h before the start of the co-culture. Donor T cells were stained with Far Red DDAO-SE (Life Technologies). MT4C5 cells were then co-cultured with MDDC at a 1:2 ratio (T:MDDC). Non-infected MT4C5 cells were used as negative controls. Co-cultures were performed for 72 h. VLPs carrying Vpx were produced as previously described (Puigdomenech et al., 2013) and added to MDDCs 2 h before HIV-1 infection and maintained during the experiment.

Origin and production of lentiviral vectors

Lentiviral TRC1 pLKO.1-puro vectors (Sigma-Aldrich, St. Louis, MO) encoding shRNA are listed in the table below and were mostly obtained from the BCCM/LMBP Plasmid collection, Department of Biomedical Molecular Biology, Ghent University, Belgium (http://bccm.belspo.be/about/lmbp.php). For knock-down of IRF3, a pLKO.1-puro vector targeting IRF3 was kindly provided by Dr. N. Manel (Institut Curie, Paris, France) (Manel et al. 2010). As a control, a pLKO.1-puro vector encoding a non-targeting scrambled shRNA (SHC-002) was purchased from Sigma-Aldrich. Lentiviruses were produced in 293T cells by transfection with the pLKO.1 vectors and the MISSION® Lentiviral Packaging Mix using FuGENE® HD Transfection Reagent (Promega,

Leiden, The Netherlands) as described before (Landi et al., 2014). Medium was refreshed 24 h after transfection. Viral supernatant was harvested after 48 h and centrifuged at 900 g for 10 min, to clarify the supernatant from remaining cells.

List of pLKO.1-puro shRNA-encoding lentiviral vectors used for knock-down of host proteins.

Origin lentiviral vector	**Target gene (official symbol)**	**Refseq**	**TRC number / reference**	**Target sequence**	**Targeted gene region**
BCCM/LMBP[a]	MB21D1	NM_138441.2	TRCN0000148694	CTGCCTTCTTTCACGTATGTA	CDS
BCCM/LMBP[a]	MB21D1 (#2)	NM_138441.2	TRCN0000149984	CAACTACGACTAAAGCCATTT	CDS
BCCM/LMBP[a]	MB21D1 (#3)	NM_138441.2	TRCN0000146282	CTTTGATAACTGCGTGACATA	CDS
BCCM/LMBP[a]	TMEM173	NM_001301738.1, NM_198282.3	TRCN0000161052	GCTGGCATGGTCATATTACAT	CDS
BCCM/LMBP[a]	TBK1	NM_013254.3	TRCN0000003182	GCAGAACGTAGATTAGCTTAT	CDS
BCCM/LMBP[a]	PQBP1 (#1)	NM_001032381.1, NM_001032382.1, NM_001032383.1, NM_001032384.1, NM_001167989.1, NM_001167990.1, NM_001167992.1, NM_005710.2, NM_144495.2, XM_005272571.3, XM_005272572.3, XM_011543884.1	TRCN0000019941	CCCTTACTACTGGAATGCAGA	CDS
BCCM/LMBP[a]	PQBP1 (#2)	NM_001032381.1, NM_001032382.1, NM_001032383.1, NM_001032384.1, NM_001167989.1, NM_001167990.1, NM_001167992.1, NM_005710.2, NM_144495.2, XM_005272571.3, XM_005272572.3, XM_011543884.1	TRCN0000019942	GAGATCATTGCCGAGGACTAT	CDS
BCCM/LMBP[a]	VPRBP (DCAF1)	NM_001171904.1, NM_014703.2	TRCN0000129579	CCTCCCATTCTTCTGCCTTTA	CDS
Dr. N. Manel, Institut Curie, Paris, France	IRF3	NM_001197125.1, NM_001197126.1, NM_001197123.1, NM_001197122.1, NM_001571.5	Manel et al. 2010	CTGCCTGGATGGCCAGTCACAC	CDS
Sigma-Aldrich	Non-targeting scrambled shRNA control (SHC-002)	Not applicable	Not applicable	Not applicable	Not applicable

Table shows official gene symbol of the shRNA targeted gene according to the HUGO Gene Nomenclature Committee database (www.genenames.org); Refseq code of the targeted transcripts (Reference sequence

database of National Center for Biotechnology Information (www.ncbi.nlm.nih.gov)); TRC number of the clone from the Sigma Mission® TRC1 lentiviral library, sequence in the gene transcript targeted by the shRNA and corresponding region in the transcripts targeted (CDS: coding sequence).
[a]Sigma Mission® TRC1 vector obtained through the BCCM/LMBP Plasmid collection, Department of Biomedical Molecular Biology, Ghent University, Belgium (http://bccm.belspo.be/about/lmbp.php)

Knock-down of host genes by lentiviral vector transduction and subsequent infection with cell-free HIV-1 or co-culture with HIV-1 infected cells

pDC depleted primary $CD4^+$ T cells were transduced immediately after isolation from peripheral blood with pLKO.1 lentiviral vectors. Cells were plated at 300,000 cells in 55 µL RPMIc per well of a 96-well flat bottom plate and 45 µL of lentiviral vector supernatant was added to each well in the presence of 20 ng/mL IL-2, 1 µg/mL PHA and 8 µg/mL polybrene. Cells were then spinoculated for 30 min, 950 g at 32 °C. After 24 h, fresh RPMIc containing IL-2 and PHA was added to the cells. 48 h after transduction puromycin (1.2 µg/mL final concentration, Sigma-Aldrich) was added to the cells. After 72 h, PHA/IL-2 stimulation was ended by removing all medium and adding fresh RPMIc containing IL-2 and puromycin. 5 days after transduction cells were counted using MACSquant® Analyzer or using Flow-count Fluorospheres (Beckman Coulter, Suarlée, Belgium) and FACSCalibur flow cytometer, according to manufacturer's instructions. For infection with cell-free HIV-1, cells were plated at $2 \times 10^5 - 2.5 \times 10^5$ cells per well of a 96-well flat bottom plate and infected by spinoculation as described above. For infection through co-culture with HIV-1 infected MT4 cells,
cells were plated at $1.2 \times 10^5 - 1.5 \times 10^5$ cells per well and an equal amount of HIV-infected or non-infected MT4 cells were added in a total volume of 200 µL fresh RPMIc (+ IL-2). Remaining primary $CD4^+$ T cells were lysed in QIAZOL prior to infection or co-culture and used for target gene expression analysis. 24 h after the start of the co-culture or 48 h after infection with cell-free HIV-1, cells were lysed in QIAZOL and used for IFN-β and/or IFIT1 expression analysis. IFN-β mRNA induction was not observed after co-culture of HIV-infected MT4 cells and primary CD4+ T cells when infection was blocked by HIV-1 reverse transcriptase inhibitor nevirapine (data not shown).
For stimulation of cells with cGAMP, cells were plated at 2.5×10^5 cells per well of a 96-well flat bottom plate and incubated with 10 µg/mL of synthetic 2',3' cGAMP (Invivogen, Toulouse, France) after pre-incubation with Lipofectamine® 2000 (Life Technologies) at a 4:1 ratio (µg cGAMP : µL Lipofectamine® 2000). 24 h after treatment, cells were lysed in QIAZOL and used for IFN-β and/or IFIT1 expression analysis.
Western Blot
For analysis of cGAS expression levels, primary CD4+ T cells transduced with shRNA-encoding vectors and selected with puromycin were lysed in Laemli sample buffer (0.125 M
Tris, pH 6.8, 25 % glycerol, 2.3 % SDS). Lysates were sheared and protein concentrations were determined by RC DC Protein Assay (Bio-Rad). Equal amounts of protein were separated on a BOLT 4–12 % Bis-Tris Plus gel (Thermo Fisher Scientific), blotted onto PVDF membranes (Invitrogen) in reducing conditions and probed with an antibody against cGAS (rabbit anti-human MB21D1; diluted 1:500, Sigma-Aldrich). Subsequently, blots were probed with HRP-conjugated donkey anti-rabbit antibody (1:4000, ECL Rabbit IgG, GE Healthcare Life Sciences, Diegem, Belgium). The signal was generated using a Super Signal West Femto Maximum Sensitivity Substrate (Thermo Fisher Scientific), detected by chemoluminescence with the ImageQuant LAS 4000 (GE Healthcare Life Sciences). For staining of ß-actin, blots were stripped with Restore Plus Western Blot stripping buffer (Thermo Fisher Scientific) according to manufacturer's instructions and probed with an anti-ß-actin antibody (mouse monoclonal ß-actin, BA3R, diluted 1:1000, Thermo Fisher Scientific). Secondary staining was performed with a HRP-conjugated sheep anti-mouse antibody (1:2000, sheep anti-mouse whole ECL antibody, GE Healthcare) and signal was generated and detected as described above.

Quantitative real-time PCR (qPCR)

RNA was isolated from QIAZOL lysates using the miRNeasy mini kit, either manually or with QIAcube (Qiagen), according to manufacturer's instructions. RNA (max. 1 µg) was subsequently treated with amplification-grade DNAse I (Life Technologies) and used for synthesis of cDNA with Superscript® III reverse transcriptase and random primers (Life Technologies), all according to manufacturer's instructions. Depending on the gene to measure, cDNA was subsequently 3x (for target genes)-15x (for reference genes) diluted by addition of Nuclease-Free Water (NFW) (Ambion, Life Technologies) and 5 µL of diluted cDNA was used as input for qPCR. For qPCR measurement of *YWHAZ*, *UBC*, *IFIT1*, IFN-α and *IRF3*, forward (FWD) and reverse (REV) primers were used at a final concentration of 300 nM in combination with 2x concentrated LightCycler® 480 SYBR Green I Master mix (Roche Diagnostics, Vilvoorde, Belgium) in a final reaction of 15 µL. For measurement of IFN-β (*IFNB1*), FWD and REV primers were used at a final concentration of 500 nM and a double-quencher probe (56-FAM/ZEN/3′ Iowa Black FQ) was used at a final concentration of 250 nM in combination with 2x concentrated LightCycler® 480 Probes Master mix (Roche Diagnostics) in a final reaction of 15 µL. Primers and probe were manufactured by IDT (Leuven, Belgium). For measurement of *MB21D1*

(cGAS), *TMEM173* (STING), *TBK1*and *PQBP1* 20x concentrated commercial Prime PCR Sybr® Green assays (Bio-Rad Laboratories, Temse, Belgium) were used in combination with 2x concentrated LightCycler® 480 SYBR Green I Master mix or 2x concentrated SsoAdvanced™ Universeal SybrGreen® Supermix (Bio-Rad Laboratories) in a final reaction of 15 µL. Primer/probe sequences or assay IDs are listed in the table below. qPCR reactions were performed in 384-well plates (LightCycler® 480 Multiwell Plates 384, white, Roche Diagnostics) on the on the LightCycler® 480 II instrument (Roche Diagnostics) using following program: 10 min at 95 °C; 45 cycles of amplification: 10 s at 95 °C, 1 min at 60 °C.
For each sample, qPCR reactions were performed in duplo. A non-template control (NFW instead of cDNA) and a serial 10-fold dilution of cDNA derived from poly I:C stimulated PBMCs (standard curve) was included for measurement of each gene on each plate. Cycles of quantification (Cq) values were generated by the LightCycler® 480 software 1.5.0 according to the second-derivative maximum method. Amplification efficiency of each qPCR assay was tested during primer/assay validation and varied from 85-105 %. Melting curve analysis was performed for the not previously validated SYBR Green assays (*IFIT1*, IFN-α and *IRF3*) and showed a single peak. Calibrated normalized relative quantities (CNRQs) were calculated for each target gene in each sample based on obtained Cq values, with the qBasePlus Software (Biogazelle, Zwijnaarde, Belgium), using *YWHAZ* and *UBC* as reference genes and using target- and run- specific amplification efficiencies. GeNorm analysis (implemented in qBase Plus) was used to select *YWHAZ* and *UBC* as stable reference genes in prior experiments.

Properties of the qPCR assays used.

Official gene symbol	**Detected Refseq transcripts**	**Primer/probe sequence source**	**Primer / probe identity**	**Primer/probe sequence**	**Ampli-con length**
YWHAZ	NM_001135702.1, NM_001135701.1, NM_001135700.1, NM_001135699.1, NM_145690.2, NM_003406.3	RTprimerDB ID: 9 (Pattyn et al., 2003)	FWD	5'-ACTTTTGGTACATTGTGGCTTCAA-3'	94
			REV	5'-CCGCCAGGACAAACCAGTAT-3'	
UBC	NM_021009.6	RtprimerDB ID: 8 (Pattyn et al., 2003)	FWD	5'-ATTTGGGTCGCGGTTCTTG-3'	133
			REV	5'-TGCCTTGACATTCTCGATGGT-3'	
IFIT1	NM_001548.4	Designed with Primer-BLAST (Ye et al., 2012)	FWD	5'-GATCTCAGAGGAGCCTGGCTAA-3'	84
			REV	5'-TGATCATCACCATTTGTACTCATGG-3'	
IFNA cluster (IFNA10	NM_002171.2, NM_021268.2, NM_021068.2,	RTprimerDB ID: 3541 (Pattyn et al., 2003)	FWD	5'-GTGAGGAAATACTTCCAAAGAATCAC-3'	93

, IFNA17, IFNA4, IFNA2, IFNA8, IFNA7, IFNA14, IFNA21, IFNA16, IFNA6, IFNA1, IFNA13, IFNA5)	NM_000605.3, NM_002170.3, NM_021057.2, NM_002172.2, NM_002175.2, NM_002173.2, NM_021002.2, NM_024013.2, NM_006900.3, NM_002169.2		REV	5'-TCTCATGATTTCTGCTCTGACAA-3'	
IFNB1	NM_002176.2	Designed with PrimerQuest Assay design IDT	FWD	5'-GCTTCTCCACTACAGCTCTTTC-3'	115
			REV	'5-CAGTATTCAAGCCTCCCATTCA-3'	
			PROBE	56-FAMTTCAGTGTC/ZEN/AGAAGCTCCTGTGGCAA/3IABkFQ	
IRF3	NM_001197125.1, NM_001197124.1, NM_001197123.1, NM_001197122.1, NM_001571.5	Viemann et al., 2011	FWD	5'-AGGCCACTGGTGCATATGTTC-3'	108
			REV	5'-CCTCTGCTAAACGCAACCCTT-3'	
MB21D1	n.a.	qHsaCID0009796 Bio-rad Laboratories	/	n.a.	110
TMEM173	n.a.	qHsaCID0010565 Bio-rad Laboratories	/	n.a.	93
TBK1	n.a.	qHsaCID0018552 Bio-rad Laboratories	/	n.a.	141
PQBP1	n.a.	qHsaCID0037960 Bio-rad Laboratories	/	n.a.	80

Table shows properties of primers used for qPCR: official gene symbol according to the HUGO Gene Nomenclature Committee database (www.genenames.org); detected Refseq transcripts are those obtained by Primer-BLAST (Ye et al., 2012) using the indicated primer sequences with default parameters; FWD: forward primerr, REV: reverse primer, n.a. not available

Measurement of secreted type 1 IFN bioactivity

HL-116 cells were plated 16 h prior to the assay at 40,000 cells per well of a 96-well-flat bottom plate in 200 µL DMEMc. Medium was removed and 100 µL culture supernatant or recombinant IFNα, together with 100 µL DMEMc was added. Cells were incubated for 7-8 h, washed with PBS and lysed (Cell Culture Lysis 5X Reagent, Promega). Lysates were either processed immediately or stored at -80°C until further use. For measurement of luciferase activity, 20 µL cell lysate was transferred to 96-well white solid plates (Costar/Corning, Amsterdam, The Netherlands) and luciferase assay was conducted using 50 µL Luciferase reagent (Luciferase Assay System, Promega) in a TriStar LB 941 automated plate reader (Berthold Technologies, Bad Wildbad, Germany). IFN-I levels are expressed in IU/mL as equivalent of IFNα1b (Immunotools, Friesoythe, Germany) bioactivity for primary $CD4^+$ T cells and as equivalent of IFNα2a (PBL Assay Science) bioactivity for MDDC experiments, both determined by inclusion of a dilution series of the recombinant IFNα in each experiment.

Measurement of MxA and HIV infection levels.

Intracellular staining for p24 or MxA in primary $CD4^+$ T cells was performed with the Fix and Perm Cell kit (AN DER GRUB Bio Research, Susteren, The Netherlands) according to manufacturer's instructions using following antibodies: HIV-1 core antigen PE (phycoerythrin)-conjugated mAb (Clone KC57, Beckman Coulter, Suarlée, Belgium) for p24 or anti-MxA (anti-MX1) (rabbit polyclonal, Abcam, Cambridge, UK)/ rabbit control serum (Cell Signaling Technology, Leiden, The Netherlands) as primary antibody and Alexa Fluor® 660 goat anti-rabbit IgG (Life Technologies) as secondary antibody for MxA. For HIV NL4-3-HSA-I infected cells, surface staining was performed with an anti-CD24-APC (allophycocyanin) antibody (HSA; mouse clone M1/69, BioLegend, San Diego, CA). Cells were analyzed by flow cytometry (FACSCalibur using CellQuest Pro software (BD Biosciences) or FlowJo 887 (Tree Star, Ashland, OR) or Flowing Software (Turku Centre for Biotechnology, University of Turku) for analysis; MACSQuant flow cytometer (Miltenyi Biotec) using MACSQuantify™ version 2.5 for analysis). Living cells were gated as propidium-iodide staining negative cells after forward scatter (FSC) and side scatter (SSC) gating. For HIV-2 CI85 infected cells, surface staining was performed with an anti-CD4-APC antibody (clone M-T466, Miltenyi Biotec). Percentage of HIV-1 infected cells was determined as percentage of HSA, GFP or p24 expressing cells and for HIV-2 CI85 as percentage of $CD4^{low}$ cells. For evaluation of HIV-1 infection levels in co-cultures, cells were stained with anti-CD3-APC antibody (clone SK7, BD Biosciences) and percentage of HIV-1 infected primary CD4+ T cells was determined by flow cytometry as percentage of GFP+ cells among $CD3^{high}$ cells.

To quantify virion release, supernatant from infected cultures was harvested and centrifuged at 350 g for 10 min, to clarify the supernatant from remaining cells. Reverse transcriptase activity in the supernatant was subsequently determined with the SG-PERT assay (as described in Vermeire et al., 2012).

To evaluate HIV-1 infection levels in MDDCs, cells were intracellularly stained with anti-HIV-Gag (KC57-PE, Beckman-Coulter) and Gag-PE and Far Red DDAO-SE levels were analyzed by flow cytometry.

Statistical analysis and software

Figures were created with Microsoft PowerPoint and GraphPad Prism 5.0 software. Statistical tests were performed with GraphPad Prism 5.0 as indicated in the figure legends.

Supplemental References

Adachi, A., Gendelman, H.E., Koenig, S., Folks, T., Willey, R., Rabson, A., and Martin, M.A. (1986). Production of acquired immunodeficiency syndrome-associated retrovirus in human and nonhuman cells transfected with an infectious molecular clone. J Virol *59*, 284-291.

Arien, K.K., Abraha, A., Quinones-Mateu, M.E., Kestens, L., Vanham, G., and Arts, E.J. (2005). The replicative fitness of primary human immunodeficiency virus type 1 (HIV-1) group M, HIV-1 group O, and HIV-2 isolates. J Virol *79*, 8979-8990.

Bachmann, M.H., Delwart, E.L., Shpaer, E.G., Lingenfelter, P., Singal, R., and Mullins, J.I. (1994). Rapid genetic characterization of HIV type 1 strains from four World Health Organization-sponsored vaccine evaluation sites using a heteroduplex mobility assay. WHO Network for HIV Isolation and Characterization. AIDS Research and Human Retroviruses *10*, 1345-1353.

Imbeault, M., Lodge, R., Ouellet, M., and Tremblay, M.J. (2009). Efficient magnetic bead-based separation of HIV-1-infected cells using an improved reporter virus system reveals that p53 up-regulation occurs exclusively in the virus-expressing cell population. Virology *393*, 160-167.

Kutsch, O., Benveniste, E.N., Shaw, G.M., and Levy, D.N. (2002). Direct and quantitative single-cell analysis of human immunodeficiency virus type 1 reactivation from latency. J Virol *76*, 8776-8786.

Landi, A., Vermeire, J., Iannucci, V., Vanderstraeten, H., Naessens, E., Bentahir, M., and Verhasselt, B. (2014). Genome-wide shRNA screening identifies host factors involved in early endocytic events for HIV-1-induced CD4 down-regulation. Retrovirology *11*, 118.

Le Rouzic, E., Morel, M., Ayinde, D., Belaidouni, N., Letienne, J., Transy, C., and Margottin-Goguet, F. (2008). Assembly with the Cul4A-DDB1DCAF1 ubiquitin ligase protects HIV-1 Vpr from proteasomal degradation. J Biol Chem *283*, 21686-21692.

Levy, D.N., Aldrovandi, G.M., Kutsch, O., and Shaw, G.M. (2004). Dynamics of HIV-1 recombination in its natural target cells. Proc Natl Acad Sci U S A *101*, 4204-4209.

Louwagie, J., McCutchan, F.E., Peeters, M., Brennan, T.P., Sanders-Buell, E., Eddy, G.A., van der Groen, G., Fransen, K., Gershy-Damet, G.M., Deleys, R., *et al.* (1993). Phylogenetic analysis of gag genes from 70 international HIV-1 isolates provides evidence for multiple genotypes. AIDS *7*, 769-780.

Pattyn, F., Speleman, F., De Paepe, A., and Vandesompele, J. (2003). RTPrimerDB: the real-time PCR primer and probe database. Nucleic Acids Research *31*, 122-123.

Rucker, E., Grivel, J.C., Munch, J., Kirchhoff, F., and Margolis, L. (2004). Vpr and Vpu are important for efficient human immunodeficiency virus type 1 replication and CD4+ T-cell depletion in human lymphoid tissue ex vivo. J Virol *78*, 12689-12693.

Schindler, M., Wurfl, S., Benaroch, P., Greenough, T.C., Daniels, R., Easterbrook, P., Brenner, M., Munch, J., and Kirchhoff, F. (2003). Down-modulation of mature major histocompatibility complex class II and up-regulation of invariant chain cell surface expression are well-conserved functions of human and simian immunodeficiency virus nef alleles. J Virol *77*, 10548-10556.

Stove, V., Van de Walle, I., Naessens, E., Coene, E., Stove, C., Plum, J., and Verhasselt, B. (2005). Human immunodeficiency virus Nef induces rapid internalization of the T-cell coreceptor CD8alphabeta. J Virol *79*, 11422-11433.

Uze, G., Di Marco, S., Mouchel-Vielh, E., Monneron, D., Bandu, M.T., Horisberger, M.A., Dorques, A., Lutfalla, G., and Mogensen, K.E. (1994). Domains of interaction between alpha interferon and its receptor components. Journal of Molecular Biology *243*, 245-257.

Van Damme, J., De Ley, M., Van Snick, J., Dinarello, C.A., and Billiau, A. (1987). The role of interferon-beta 1 and the 26-kDa protein (interferon-beta 2) as mediators of the antiviral effect of interleukin 1 and tumor necrosis factor. J Immunol *139*, 1867-1872.

Vermeire, J., Naessens, E., Vanderstraeten, H., Landi, A., Iannucci, V., Van Nuffel, A., Taghon, T., Pizzato, M., and Verhasselt, B. (2012). Quantification of reverse transcriptase activity by real-time PCR as a fast and accurate method for titration of HIV, lenti- and retroviral vectors. PLoS One *7*, e50859.

Viemann, D., Schmolke, M., Lueken, A., Boergeling, Y., Friesenhagen, J., Wittkowski, H., Ludwig, S., and Roth, J. (2011). H5N1 virus activates signaling pathways in human endothelial cells resulting in a specific imbalanced inflammatory response. J Immunol *186*, 164-173.

Ye, J., Coulouris, G., Zaretskaya, I., Cutcutache, I., Rozen, S., and Madden, T.L. (2012). Primer-BLAST: a tool to design target-specific primers for polymerase chain reaction. BMC Bioinformatics *13*, 134.